IEEE Access
Multidisciplinary ⋮ Rapid Review ⋮ Open Access Journal

Received 6 June 2023, accepted 20 June 2023, date of publication 23 June 2023, date of current version 28 August 2023.

Digital Object Identifier 10.1109/ACCESS.2023.3289005

SURVEY

Physical Realization of Measurement Based Quantum Computation

MUHAMMAD KASHIF AND SAIF AL-KUWARI, (Senior Member, IEEE)
Division of Information and Computing Technology, College of Science and Engineering, Hamad Bin Khalifa University, Qatar Foundation, Doha, Qatar
Corresponding author: Muhammad Kashif (mkashif@hbku.edu.qa)

ABSTRACT Quantum computers, leveraging the principles of quantum mechanics, hold the potential to surpass classical computers in numerous applications, with implications across various domains. Besides the well-known gate model, Measurement-based Quantum Computation (MBQC) is another promising computational approach to achieve universal quantum computation. In MBQC, large ensembles of qubits are prepared in a highly entangled cluster state, forming the basis for executing quantum computations through sequential measurements. Cluster states are realized using both continuous variables (CV) and discrete variables (DV) techniques. In the CV-based methods, Frequency Domain Multiplexing (FDM), Time Domain Multiplexing (TDM), Spatial Domain Multiplexing (SDM), and hybrid schemes are employed. This paper thoroughly discusses and compares these approaches, elucidating their strengths and limitations. Additionally, the generation of photonic cluster states in DV is explored and some recent results are reported. Some recent state-of-the-art advancements in photonic and superconducting qubits entanglement, which can potentially serve as cluster states, are also presented. Finally, we highlight the approach that exhibits the most promising characteristics for achieving efficient cluster state realization in the context of MBQC.

INDEX TERMS Continuous variables cluster states, discrete variables cluster states, measurement based quantum computation, one-way quantum computation, physical realization, quantum computation.

I. INTRODUCTION

The race to achieve advanced computational capabilities originated during the Second World War with the introduction of Alan Turing's Universal Turing Machine, marking the advent of the first general-purpose digital computer equipped with an electronically stored program [1]. In 1945, Von Neumann further refined Turing's concept, introducing modifications that led to the development of the most widely adopted computer architecture employed by the majority of modern computers. This architecture has demonstrated exceptional efficiency in addressing a broad range of significant problems [2]. However, the continued miniaturization of electronic components in conventional computers has reached a point where quantum effects arising during the fabrication process are beginning to disrupt the functionality of these devices. This predicament has raised concerns about the sustainability of Moore's law [3], which posits that computational power doubles approximately every 18 months. Furthermore, there exist certain problems that cannot be feasibly solved within practical time frames using classical computers, even if Moore's law persists [2]. Consequently, the need for a novel approach to computation has become evident, leading to the emergence of quantum computation as a promising solution.

In the 1980s, Richard Feynman was among the pioneers who advocated the potential of quantum computers to efficiently solve computationally intensive problems in physics and chemistry [4]. Quantum computing is a promising computational paradigm that harnesses the principles of quantum mechanics [2], enabling the execution of certain tasks substantially faster than the classical computers [5]. In 1994, Peter Shor discovered a quantum algorithm capable of efficiently solving mathematical problems at the heart of modern cryptography, thereby posing a potential threat to public-key cryptography [6]. Similarly, in 1996, Lov Grover proposed a quantum search algorithm [7], that exhibits polynomial time complexity, surpassing the efficiency of any classical computer for searching through unstructured data. Several other

The associate editor coordinating the review of this manuscript and approving it for publication was Wei Huang.

quantum algorithms [8], [9], [10] further demonstrated this quantum advantage and established that classical algorithms cannot achieve comparable performance.

Since then, the quest for developing a practical quantum computer has commenced, and significant progress has been made to date. Notably, recent advancements have provided a tangible demonstration of quantum advantage through the achievement of Quantum Supremacy [5], [11], [12]. In this landmark achievement, a real quantum computer successfully performed a task within seconds that would necessitate thousands of years for a super (classical) computer to accomplish.

A key distinction between classical computers and quantum computers lies in the concept of state [13]. While classical computers employ classical bits to store and manipulate information, quantum computers utilize quantum bits, known as qubits, for the representing and manipulating the quantum information.

A qubit can be realized using any two-level quantum system, such as the spin of a particle or the polarization of a photon [14]. The two levels of a qubit correspond to its basis states, typically denoted as $|0\rangle$ and $|1\rangle$. However, unlike classical bits, qubits can exist in a superposition of both states simultaneously [3]. The notion that a continuum classical bit can be represented by a combination of 0 and 1 is a common conjecture. However, it is important to recognize that qubit superposition and continuum classical bits are fundamentally distinct concepts in the fields of computing and information theory. A continuum classical bit, as the name suggests, implies a continuous range of values for representing information. This aligns more closely with analog systems, where values can span across a continuous spectrum. In contrast, a qubit in superposition represents information within a quantum mechanical framework, allowing it to exist as a combination of multiple states simultaneously. Furthermore, continuum classical bits typically rely on an analog encoding scheme, where the information is represented by a physical quantity, such as voltage or position, that can vary continuously. In contrast, qubits are usually encoded using discrete quantum states, such as the polarization of a photon or the spin of an electron. The superposition of qubits emerges from the principles of quantum mechanics.This superposition property allows quantum computers to perform parallel computations and explore multiple possibilities simultaneously. Furthermore, qubits also possess the property of entanglement. Entanglement allows multiple qubits to become correlated in such a way that the state of one qubit is inherently linked to the state of another, regardless of their spatial separation [2], [15]. This feature enables quantum computers to perform certain computations with a higher efficiency compared to classical computers.

A. TYPES OF QUANTUM COMPUTATION

Quantum computation can be broadly divided into two categories: Adiabatic quantum computation (quantum annealing) and Universal quantum computation. Adiabetic quantum computation does not use qubit gates, instead analog values are manipulated in Hamiltonian [2]. Hamiltonian of a system in quantum mechanics is an operator representing the total energy of the system (potential and kinetic energy). On the other hand universal quantum computation can be achieved through various approaches, however, the most prominent is gate-based quantum computation.[1]

1) ADIABATIC QUANTUM COMPUTATION

Adiabatic quantum computation is an analog quantum computation technique where qubits with initial quantum states are changed to Hamiltonian in a way that the problem to be solved is encoded in the final Hamiltonian, which corresponds to the output [16]. The adiabatic quantum computation refers to a phenomenon when the system remains in the ground state of changing Hamiltonian [13]. Adiabatic quantum computation exploits quantum annealing for solving optimization problems for various applications including machine learning [17], [18], [19], classification tasks [20], variational auto-encoders [21], [22] and compressive sensing [23]. Every qubit state can be represented as an energy level in quantum annealers. These states are simulated for a given application and the lowest energy results are obtained. The optimal solution is provided by a state with lowest energy. Adiabatic quantum computers are among the first commercially available quantum computers, mainly popularized by D-wave Systems [24], which develops programmable quantum annealers.

2) UNIVERSAL QUANTUM COMPUTATION

Universal quantum computers can complete tasks that are beyond the reach of current classical computers [2]. Gate-based quantum computation is one of the most-widely used approaches for universal quantum computation and uses quantum gates to perform operations on qubits. This approach often use the quantum circuit model [2] to perform a sequence of operations and measurements on qubits. IBM and google (and many other industry giants and startups) have already built gate-based quantum computer with around 100 qubits [13], [25]. Building universal quantum computers with sufficiently large number of qubits, typically thousands of qubits, is quite challenging, but when built they are anticipated to solve highly computationally intensive tasks within practical amount of time. Furthermore, the advent of universal quantum computers is anticipated to revolutionize numerous applications, particularly machine learning, which is often referred to as quantum machine learning (QML) [26], [27], [28], [29], [30], [31]. QML is an emerging research area that holds immense potential for harnessing the power of quantum computing to solve complex problems and unlock new possibilities [32], [33]. While QML is a highly active field experiencing rapid advancements, it is important to note that this survey paper does not delve into the specifics

[1] Adiabatic and gate-based quantum computation have shown to be equivalent but are not the same class of quantum computation.

QML. Instead, it focuses on categorization of the approaches used for physical realization of measurement based quantum computation, and recent state-of-the-art comparison.

B. REQUIREMENTS AND APPROACHES FOR UNIVERSAL QUANTUM COMPUTING AND QUANTUM INFORMATION PROCESSING

To realize a universal quantum computer, the generation of reversible and deterministic entanglement is a fundamental requirement. Early efforts in the field focused on entangling closely located qubits, typically nanometers apart [34], [35] However, achieving close proximity without compromising individual qubit control poses significant challenges and scalability limitations [36]. To overcome this issue, Raussendorf and Briegel proposed an alternative approach in 2001, known as measurement-based quantum computation (MBQC) [37]. MBQC relies on exploiting qubit measurements in different bases using a highly entangled resource state, enabling quantum computations without direct qubit entanglement operations. We discuss more details about MBQC in section II.

Quantum gates with high fidelity rates[2] are key to efficient quantum information processing (QIP) [3], which are directly affected by control imperfections and decoherence.[3] Upgrading the fabrication processes can mitigate the decoherence [40], but this requires extensive research at the material that is being used to realize qubits [41], [42]. It is important to note that MBQC is not inherently immune to decoherence. The techniques such as error correction, error mitigation techniques, fault-tolerant designs, and error-resilient measurement patterns can help enhance its resilience and improve the overall reliability of quantum computations. Control imperfections, including signal distortion and instrumental instability, can be mitigated by using exquisite and complex calibration processes [5]. The fidelity rate of quantum gates is usually measured via randomized benchmarking [43].

Functional quantum computers, most notably based on superconducting qubits, have already been developed(though with limited number of qubits, < 100). However, in order to fully utilize the computational power of quantum computation, a significantly large (tens of thousands) number of qubits are required [44], and because of the above-mentioned limitations scaling up beyond ''quantum supremacy'' is experimentally challenging in existing quantum computers. This is where MBQC may prove an advantage. Cluster or graph states, which are building blocks of MBQC [45], have shown entanglement robustness against decoherence [46]. Hence the MBQC, sometimes also referred as cluster state model, is well suited for scalable quantum computation and advances in research have already been made for physical realization of cluster states [47], [48], [49], [50], [51].

[2]Fidelity rate is measure of similarity between two quantum states [38].

[3]Decoherence is the loss of quantum coherence that makes the qubit entangled with the environment resulting in an inaccurate quantum computation [39].

C. RELATED WORK

Earlier proposals on MBQC were mostly focusing on general MBQC, its universality proof and its potential in achieving scalable quantum computation model. However, in recent years, there has been a noticeable shift towards experimental efforts to demonstrate the feasibility of MBQC through the creation and manipulation of cluster states. There are various review papers on physical realization of quantum computers [52], [53], [54], [55]. However, despite its potential, there is no dedicated work in the literature surveying the state-of-the-art physical realizations of MBQC except [56], which only reviews one of subtypes of MBQC's physical realization techniques (Frequency domain multiplexing) for continuous variables cluster states. A recent review on general MBQC is published in [57], with no focus on physical realization. A brief scope comparison of our survey with some recent related surveys is presented in Table 1. Hence, a detailed review of the approaches being used for implementing cluster states for MBQC, is the ultimate need of time providing the research community a sound overview of what has been achieved in this regard and what potentially can be achieved.

D. CONTRIBUTION AND SCOPE

This paper presents a detailed investigation into the techniques and approaches utilized for the physical realization of Measurement-Based Quantum Computation (MBQC), following an initial discussion on MBQC and its universality. The main focus lies on two primary approaches: Continuous Variables (CV) and Discrete Variables (DV), both employed for the realization of cluster states. Within the CV-based approaches, we further categorize them into four subcategories: frequency domain multiplexing, time domain multiplexing, spatial domain multiplexing, and hybrid techniques that combine two multiplexing approaches. A thorough comparison of recent state-of-the-art proposals is provided for each of these techniques. Additionally, the current advancements in DV-based cluster state realization, particularly in photonic qubits, are summarized and compared. Furthermore, we survey and compare recent progress in DV-based qubit entanglement, specifically focusing on photonic and superconducting qubits, which have the potential to serve as resource states for MBQC. An abstract view of our contributions is illustrated in Figure 1.

E. ORGANIZATION

The rest of this paper is organized as follows: Section II provides an overview of MBQC and the role of cluster states in MBQC. Universality of MBQC is discussed in this section too. Section IV provides a general overview of the main approaches of physically realizing MBQC. This is followed by Sections V and VI, where we discuss in detail the main approaches adopted for physical realization of MBQC, namely the CV-based and DV-based quantum, respectively. These sections also report on the existing experimental results of such approaches. Finally, the paper concludes

TABLE 1. Scope comparison of this survey with recent surveys on MBQC.

Ref#	CV physical realization of cluster states				DV physical realization of cluster states
	FDM	TDM	SDM	Hybrid	
[56]	✓	×	×	×	×
[57]	×	×	×	×	×
Ours	✓	✓	✓	✓	✓

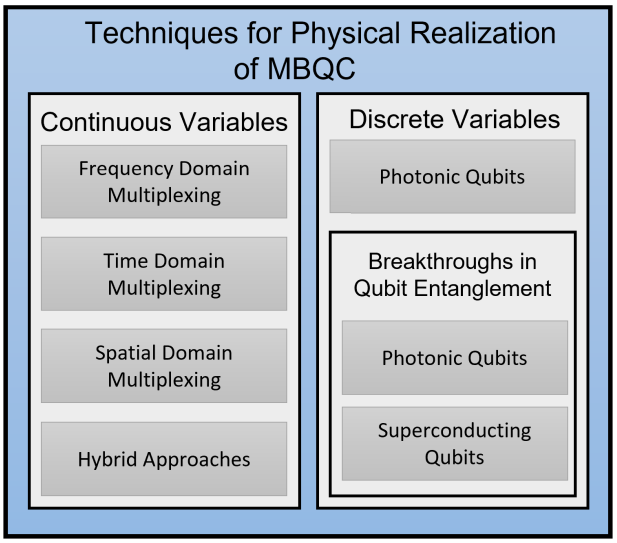

FIGURE 1. Our contributions.

in Section VII, where we provide some concluding remarks and point out some promising directions toward realizing a practical a quantum computer based on MBQC.

II. MEASUREMENT BASED QUANTUM COMPUTATION (MBQC)

In MBQC, all the computations are performed via measurements by exploiting a highly entangled resource state (also called cluster state). The two well-known schemes for MBQC are one-way quantum computation (1WQC) model and teleportation-based model. In 1WQC, single qubit measurements are used whereas joint measurements (entangled measurements) are used in teleportation-based model to achieve universal quantum computation [58].

Moreover, in teleportation-based model, all the qubits present in the system are measured separately in a specific order and measurement basis, which specify the actual algorithm. On the other hand, in 1WQC, generation of entanglement is no longer part of the quantum algorithm being developed. In 1WQC, the execution of an algorithm is done via measurements only, by exploiting a pre-generated entangled state [36], [59]. The system is prepared in a highly entangled quantum state known as cluster state with no dependence on the quantum algorithm being developed [58]. This study focuses on 1WQC scheme of MBQC.[4]

[4]From this point onwards MBQC and 1WQC are interchangeably used.

However, readers interested about teleportation-based model are referred to [60].

A typical workflow of 1WQC begins by creating such cluster state, encoding the information onto the cluster state and finally perform information read-out via single-qubit measurements [49]. It is also called one-way quantum computer because the resource state entanglement can only be measured once, after which it will be destroyed [61]. Cluster states can be created by using quantum-Ising type interaction in lattice configuration between two-state particles. More details on cluster states are in Section II-A. A typical representation of MBQC, as in original paper [37], is shown in Fig. 2.

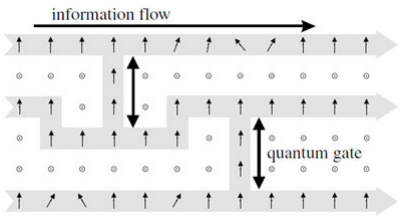

FIGURE 2. Quantum information processing in MBQC [37]. The tilted arrows represent measurement in x-y plane, vertical arrows represent measurements in the eigen basis of σ^x and circle represent measurements in the eigen basis of σ^y.

When it comes to the development of universal quantum computer, 1WQC, promise comparable potential to that of the circuit-based model which is reversible in nature [62]. In MBQC, quantum information is processed by performing a sequence of adaptive measurements [58]. For details on how adaptive measurements are performed, refer to [60]. MBQC/1WQC offers a number of advantages that makes it a potential approach to build real scalable quantum computer.

- In MBQC, typically one-way quantum computation, an entangled state is generated separately well in advance, which makes it fault-tolerant, as errors can be recognized without harming the algorithm being implemented [58].
- In 1WQC, the entire computation resource is provided by specific entangled state, allowing to track the computations all the way back to the entangled resource state, which may help in maximizing the computational advantage of quantum computation [37].
- MBQC only requires nearest-neighbor Ising coupling rather than tunable interactions between qubits which makes it more scalable and parallelized [61]

- An appropriate combination of MBQC and topological error correction provides strong basis towards noise resilient scalable quantum computer [58]. Details of error correction is not within the scope of this review.

On the other hand, compared to the circuit model, MBQC requires a relatively large number of qubits to be stored at the same time. However, 'on the fly' (Section V-A) creation of cluster states can help in overcoming this issue.

A. CLUSTER STATES

As computation in MBQC is dependent on cluster state, it is vital to shed some light on them. The term cluster state, originally penned by Raussendorf and Briegel [63], is a group of highly entangled quantum states, exhibiting two very prominent characteristics: entanglement persistency and maximal connectedness of the entangled state. Entanglement persistency is the ratio of amount of entanglement in multi-particle system to operational effort for destruction of all the entanglement in the system. Maximal connectedness means that by using single-qubit measurements, every qubit pair can be projected with certainty to maximally entangled state. Later on, as described in section (II), it was shown in [37], that 1WQC can be built using these cluster states by exploiting single-qubit measurements only.

Since the entanglement cannot be added to the system by single qubit operations, it can be inferred that in order to generate any type of entanglement from the resource state, it is essential that the resource cluster state already contains that entanglement, which can be measured using an appropriate entanglement measurement [64]. This means that maximally entangled states is what makes a resource and/or cluster state universal [65], [66], which helps to determine the potential cluster states for MBQC. Moreover, these cluster states should be multi-partite entangled states.

Although states like Dicke states, certain ground states of strongly correlated 1D spin systems, W-states and and λ-particle 1D cluster states are considered highly entangled states, they are not universal in this regard [65] because of the fact that there exist at least one non-maximal type of entanglement in these states. However, there are some states which can be universal cluster states for MBQC since they fulfill all the entanglement criteria. These states include graph states [67], which are combined with triangular, hexagonal, Kagome kinds of regular 2D lattices. Also, the lattices with high degree of defects can serve as universal cluster state for MBQC [65]. Cluster states can be visualized as a graph, sometimes called graph states. Graph states can be defined as graph with a set of vertices and edges connect the pair of vertices [61], [67]. Cluster states are subclass of graph states with an n-dimensional square grid as an underlying graph [49]. Preforming computation on cluster state proceeds in three steps [59]: (1) Preparation of cluster state, which is highly entangled many-qubit state; (2) Processing the cluster via an adaptive sequence of single-qubit measurements; (3) Using the remaining qubits for result read-out of the underlying computation. Below, we will discuss procedures for cluster states generation and preparation, measurement processing and output in cluster states.

1) CLUSTER STATE GENERATION AND PREPARATION

In context of MBQC, an n qubit cluster state can be generated by exploiting any two-dimensional (2D) and/or one-dimensional (1D) lattice graph with n number of vertices [59], as shown in Fig. 3, where a single qubit is assigned to each vertex. Once generated, a possible approach for cluster state preparation is presented in [3], according to which the following two steps can be performed for cluster state preparation: (1) Preparing all the qubits in superposition state, i.e., $|+\rangle = \frac{1}{\sqrt{2}}(|0\rangle + |1\rangle)$; (2) Apply controlled-phase gates between the two connected qubits. The order of these gates is irrelevant since these gates commute [62].

FIGURE 3. Cluster states generation and preparation (a) 1D cluster state. The circles represent qubit states and the line between two circles represents the controlled-phase operation between the corresponding qubits. (b) 2D cluster state.

2) MEASUREMENT PROCESSING AND OUTPUT IN CLUSTER STATES

The next step after preparing the cluster state is performing a sequence of processing measurements with following attributes [68]: (1) All measurements are single qubit measurements; (2) Previous measurement results may help in selecting the measurement basis - allowed to exploit feedforward of classical measurement (3) A classical computer can process these measurement results.

Once processing is completed, the outcome of the computation can be returned in two ways [59], [68]: (1) Quantum state $|\psi\rangle$ as outcome: once the processing measurement sequence is completed, output the state of remaining qubits (not measured); (2) Adding a set of read-out measurements: single-qubit measurement sequence is applied to the remaining qubits after the completion of all processing (result is a classical bit string).

B. STABILIZER FORMALISM

The number of parameters required to describe quantum states increases exponentially with the number of qubits, making the underlying quantum system more complex and difficult to understand [69]. This problem motivate investigating techniques that can help understanding these complex quantum systems. The stabilizer formalism [70], is one such technique which helps in understanding the complex quantum systems and underlying operations primarily because of the compact description and characterization of quantum states

and sub-spaces over multiple qubits, and their evolution under Pauli measurements[5] and Clifford group[6] [71].

Instead of components (in some basis), of the state itself, the stabilizer formalism specifies a set of eigenvalue relations to describe a state of a quantum system. A stabilizer can then be defined as follows [49]: An operator K is said to be stabilizer for a sub-space S when $K|\psi\rangle = |\psi\rangle$ for all $|\psi\rangle \in S$, that is $|\psi\rangle$ is an eigenstate of K with eigenvalue $+1$. It is important to note here that joint eignenstates with eigenvalues of -1 also exists, however by definition, only the eigenstates with eigenvalue of $+1$ are stabilized.

The objective in stabilizer formalism is to come up with a set of operators which not only have the stabilizing property mentioned above, but are also Hermitian members of Pauli group. Identification of stabilizing operators which uniquely defines the given state or sub-space (no state outside the sub-space), is key in stabilizer formalism, and these uniquely defined states/sub-spaces are called stabilizers states/subspaces [49]. These operators exhibit all properties of the states allowing an easier analysis of how a given state changes under unitary evolution and measurements. The set of operators stabilizing a sub-space has a group structure (also known as stabilizer group), because the product of two stabilizing operators is itself stabilizing. In quantum information processing, stabilizer states and subspaces occur in many states including GHZ states, Bell states, different error correcting codes, cluster states and graph states.

The stabilizer formalism was originally proposed for describing quantum error correction codes but it is also applicable to MBQC. Conventionally, 2^n complex number are required for a complete description of an n-qubit state. However, a group of n stabilizers can describe an n-qubit state, which is stabilized by Pauli group [70]. In other words, an entire set of commuting observables can be created by n stabilizers, resulting in a more compact description of a quantum system. Moreover, the stabilizer formalism can efficiently describe the underlying unitary evolution of Clifford Group operators. More importantly, the stabilizer formalism has proven to be quite efficient for state description of a multi-qubit system under projective measurements in X, Y and Z basis [71].

C. UNIVERSALITY OF MBQC

In order to perform arbitrary quantum computations, single and multi-qubit quantum gates are required. Any quantum approach that can realize the universal set of quantum gates can be considered a universal quantum computation approach. MBQC has been proven to be universal, with realization of universal set of single and multi-qubit gates [61]. Below we discuss the realization procedures of H-gate, $\pi/2$ gate and CNOT gate on MBQC, which, together, can form any quantum gate. The universality of MBQC has recently been demonstrated in Qiskit (an open-source software development kit for working with quantum computers at the level of circuits, pulses, and algorithms) [72] opening doors to explore MBQC while exploiting the existing gate-based quantum simulators unless a dedicated MBQC-based qubit simulator is developed.

1) HADAMARD GATE REALIZATION

Hadamard gate is an important single qubit gate in quantum Computation responsible for putting a given qubit state in superposition. In MBQC realm, the H-gate can be realized by performing these steps (the corresponding graph representation as presented by [61] is shown in Fig. 4a): (1) Prepare all qubits in the $|+\rangle$ state except the first qubit (the input qubit on Fig. 4a); (2) Entangle the connected qubits using CZ gate; (3) Measure the first Qubit in eigen basis of σ^x and measure qubits 2-4 in eigen basis of σ^y.

Once the sequence of measurements being applied on qubits 1-4, the output qubit from Fig. 4a goes to superposition state.

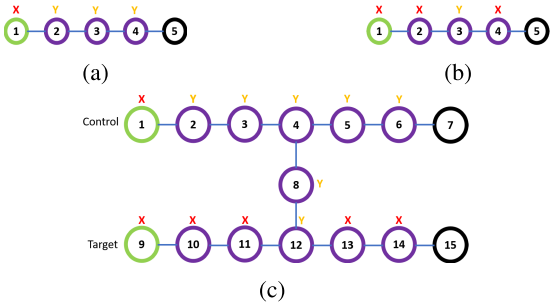

FIGURE 4. Graph state representation of H $\pi/2$ and CNOT-Gate. The circles represents the qubits, the blue lines represent the CZ operation, the green and black circles indicates the input and output qubits, respectively. The symbols *X* and *Y* represent the measurement-bases for the corresponding qubit measurement. (a) H-gate representation; (b) $\pi/2$-phase gate realization using MBQC; (c) CNOT representation.

2) $\pi/2$-PHASE GATE REALIZATION

Another important single qubit gate is $\pi/2$-phase gate. Similar to H-gate, $\pi/2$-phase gate can also be realized on MBQC with five qubits in linear configuration, but with slightly different qubit measurement basis. Fig. 4b depicts the corresponding cluster state. $\pi/2$-phase gate is prepared as follows: (1) Prepare all qubits in the $|+\rangle$ state except the first Qubit (the input qubit on Fig. 4b); (2) Entangle the connected qubits using CZ gate; (3) Measure qubits 1,2 and 4 in eigen basis of σ^x and measure the third qubit in eigen basis of σ^y. After the sequence of measurements being applied on qubits 1-4, the phase of output qubit from Fig. 4b is rotated $\pi/2$ times.

3) CNOT GATE REALIZATION

The CNOT operation can be realized in MBQC with 2D cluster state as shown in Fig. 4c. The steps required for CNOT gate realization are as follows: (1) Prepare all qubits in $|+\rangle$

[5]Pauli measurements correspond to Pauli matrices (X, Y and Z) in quantum computation.

[6]A collection of unitary operators that map Pauli group (a group comprising tensor product of Pauli matrices n times) onto itself is known as Clifford group for n qubits.

state except input qubits (1 and 9) from Fig. 4c; (2) Entangle all the connected qubits from Fig. 4c using CZ gate; (3) The output qubits (7 and 15) are not measured. The qubits 1,9,10,11,13 and 14 are measured in eigen basis of σ^x and all remaining qubits in eigen basis of σ^y.

III. INHERENT EXCLUSION OF UNPHYSICAL STATES IN MBQC

In MBQC, the computation is performed by making a sequence of measurements on individual qubits in the resource state, guided by a measurement pattern or graph structure.

The unphysical states, or the states that are not valid quantum states, are inherently excluded by the measurement process due to the following:

- **Resource State Preparation:** The initial resource state used in MBQC is carefully prepared, typically through entanglement generation techniques. This preparation process ensures that the resulting state is a valid quantum state, satisfying the necessary requirements such as unitarity and proper normalization.
- **Measurement Selection:** In MBQC, measurements are performed on individual qubits in the resource state according to a predetermined measurement pattern. These measurements correspond to specific observables and are chosen based on the desired computation. Each measurement outcome is a valid quantum state projection corresponding to the measured observable.
- **Conditional State Updates:** The measurement outcomes determine how subsequent measurements are performed and how the computation progresses. Each measurement outcome updates the state of the remaining qubits in a conditional manner. These updates ensure that only valid quantum states consistent with the measurement results are considered at each step.

By relying on the measurement outcomes and their conditional updates, MBQC effectively excludes unphysical states. The measurements guide the computation in a way that enforces the rules of quantum mechanics, ensuring that the resulting state remains a valid quantum state throughout the computation.

IV. PHYSICAL REALIZATION OF MBQC

Measurements and entanglement are the core properties MBQC relies on. In fact, the 1WQC completely relies on single-qubit measurements and entanglement between qubits, as discussed in Section II. Entanglement is provided well in advance via a highly entangled cluster state, which is a central resource of quantum information processing. Hence, the physical realization of MBQC is highly dependent on how the cluster states are being physically realized. In 1WQC, adaptive single-qubit measurements are performed to implement a certain algorithm with feed-forward operations governed by previous qubit measurement outcomes [37]. Two different feed-forward operations can be considered: previous measurement outcomes direct the selection of new measurement basis and the feed-forward corrections based on Pauli matrix on the output state [48].

1WQC is originally proposed by Raussendorf and Briegel for discrete variables [37], and is later extended to CV domain by Menicucci [73]. In DV, observables are usually realized on single-photon states known as photonic qubits [74], while in CV observables are usually realized on optical modes also known as qumodes [75]. The degree of scalability for an effective QIP is the main obstacle towards the physical realization of cluster states. The scalability, at material level, deals with the limitations on the topology and size of cluster states [76]. This limitation directly restricts the number of logical operations needed to process large volumes of data. The nature of such limitations varies depending on the materials used to physically realize qubits in a cluster state. As mentioned in Section I, the physical realization approaches for cluster states realization in MBQC context can be broadly divided into two classes: continuous variables [77], [78], [79], [80], [81] and discrete variables [76], [82], [83] cluster states.

The structure of cluster state of qubits (for DV based quantum computation) or qumodes (for CV-based quantum computation), determines the computational characterstics of MBQC [84]. One-dimensional (1D) cluster states are capable of single qubit or single qumode operations. However, two-dimensional (2D) cluster states are key for universal quantum computation. Unlike 1D, where qubits/qumodes are entangled as a single chain, in 2D cluster state,qubits/qumodes are entangled in a 2D lattice configuration. The number of qubits or qumodes determines the cluster state scalability or the number of operations. Consequently, for universal MBQC, realization of a large-scale two-dimensional cluster state is important. 2D qubit-cluster states, despite being proposed on various physical systems [81], [85], [86], [87], [88], [89], [90], is quite challenging to implement experimentally. For instance, in case of stationary qubits [81], [90], such as ion traps and superconducting qubits, a large number of qubits are required to be prepared and spatially arranged for a large-scale cluster state realization. As a result, the experimental complexity increases directly with increase of the number of qubits and cluster state dimension. Qumodes overcome these issues and for a CV optical system, qumodes, offers rich degrees of freedom and are able to deterministically generate the entanglement.

In the rest of this survey, we discuss in details the various approaches adopted in physically realizing MBQC (in both CV and DV) and report on their experimental results.

V. CV-BASED QUANTUM COMPUTATION

Quantum computation based on continuous variables relies on the promising attribute of optical parametric oscillators (OPOs) which are capable of producing significantly large number of quantum fields [91], [92], ranging from thousands to millions of quantum modes, usually termed

as qumodes [73], [93], [94] in time [85], [86], and frequency [95], [96], [97], [98] domain multiplexing. CV-based quantum computation was proposed in 1999 by Lloyd and Braunestein [99], which improves fault tolerance and quantum error correction [73], [100], while maintaining the computational advantage of universal quantum computation.

a: STATE REPRESENTATIONS

Conventional quantum computation uses Discrete Variables (DV), where qubit is the basic information unit. The qubit is a two-level system, i.e., a two-dimensional Hilbert space with computational basis states $|0\rangle$ and $|1\rangle$. The conjugate bases states for computational basis states are $|+\rangle$ and $|-\rangle$. These two bases are related by Hadamard operation H. In CV based quantum computation the basic information unit is qumode[7] [77]. Unlike qubit, qumode has Hilbert space with infinite dimensions, which is spanned by continuum of orthogonal states $|s\rangle_q$, where each $s \in \mathbb{R}$. The orthogonality condition is $\langle r|_q |s\rangle_q = \delta(r-s)$. The conjugate basis states are labelled as $|s\rangle_q$. The relation between the two bases $|s\rangle_q$ is represented by Fourier transform operation, in (1).

$$|s\rangle_p = \frac{1}{2\pi}\int_{-\infty}^{\infty} dr e^{-irs}\,|r\rangle_q = F\,|s\rangle_q$$
$$|s\rangle_q = \frac{1}{2\pi}\int_{-\infty}^{\infty} dr e^{-irs}\,|r\rangle_p = F^\dagger\,|s\rangle_p \tag{1}$$

Equation (1) also defines the unitary operator F. Qubits can be directly encoded as qumodes to perform quantum computation, such as coherent state encoding [101], or GKP encoding [102]. However, qumodes can also be used directly for any kind of CV based quantum computation [99]. The corresponding observables in CV-based quantum computation can be defined as momentum $\hat{p}$ and position $\hat{q}$, where $\hat{p}\,|s\rangle_p = s\,|s\rangle_p$ and $\hat{q}\,|s\rangle_q = s\,|s\rangle_q$ with $[\hat{q}, \hat{p} = i]$, where $-\hat{q}$ generates the positive translations in momentum and positive translations in position are generated by $\hat{p}$. Hence, an arbitrary position and momentum eigenstate can be written as in (2), where $X(s) = e^{-is\hat{p}}$ represents displacements in computational bases and $Z(s) = e^{-is\hat{q}}$ represents displacements in conjugate bases. The superposition of either $|s\rangle_p$ or $|s\rangle_q$ can form an arbitrary quantum state $|\phi\rangle$ of a CV system.

$$|s\rangle_q = X(s)\,|0\rangle_q\,, \quad |s\rangle_p = Z(s)\,|0\rangle_p \tag{2}$$

The computational basis or its conjugate is not countable, however, an arbitrary physical state $|\phi\rangle$ can be decomposed into countable infinite basis. For instance, Fock basis of definite particle number $\{|0\rangle, |1\rangle, \ldots.\}$can be used for quantum optical fields or particles in harmonic trap, where $\hat{n} = \hat{a}^\dagger\hat{a}$ is the number operator with $\hat{n}\,|n\rangle = n\,|n\rangle$, the usual bosonic operator $[\hat{a}, \hat{a}^\dagger] = 1$ and $\hat{a} = (\hat{q} + i\hat{p})/\sqrt{2}$.

[7]We will also often refer to qumode as entangled modes, modes or flying qubits in this paper.

b: VACUUM AND SQUEEZED STATES

In the context of quantum optics (which is the most widely used paradigm for the realization of CV based quantum computation), for a given mode, $\hat{p}$ and $\hat{q}$ represent the momentum quadrature and position quadrature, respectively [77]. By minimizing the quadrature deviations product ($\Delta p \Delta q = 1/2$), the qumode state has the minimum uncertainty. The vacuum or ground state $|0\rangle$, defined by $\hat{a}\,|0\rangle = 0$ is of significant importance here both theoretically and practically. it also represents the Gaussian superposition centered about 0 in computational or conjugate basis.

$$|0\rangle = \frac{1}{\pi^{1/4}}\int ds e^{-s^2/2}\,|s\rangle_q = \frac{1}{\pi^{1/4}}\int ds e^{-s^2/2}\,|s\rangle_p \tag{3}$$

The quadratures of vacuum state exhibit gaussian statistics and hence is a typical example of Gaussian state. The Einstein-Podolsky-Rosen (EPR) states are CV equivalent of bell states in qubit-based cluster states [56], where the summation of bell states is transformed to indefinite integral, which provides an intuition that EPR states are unphysical because they have infinite energy. However, it is possible to experimentally realize an approximation of these states, usually referred to as two-mode squeezed (TMS) states [103]. The OPAs can directly create such states, for instance a doubly resonant OPO below threshold [103], [104]. However, for vacuum states, finitely squeezed variance can be achieved [56], and are used widely for cluster states realization in CV-based quantum computation.

An arbitrary Gaussian state is completely determined by the first and second moments of quadrature, and Wigner function is a quite handy tool for its description. By definition, any state with Gaussian Wigner function is a Gaussian state. Wigner function [77] can efficiently describe the qumode states (however, since a cluster state realized by continuous variables is multi-mode state, a multi-mode Wigner function is used).

c: CLUSTER STATES IN CV

1WQC is based on cluster states which includes the entire entanglement resource needed for the computation, which is then governed by single qubit measurements. The canonical way of cluster states realization (using controlled phase (CZ) gate for entangling two neighboring qubits), in qubit-based quantum computation, are explained in Section II-A1

1WQC using CV based cluster states has been formulated in [73] and [77]. Moreover, in a recent survey on CV based cluster states [56], a comparison between qumode and qubit-based quantum computation is presented, following which, the cluster state for 1WQC can be created quite easily for CV based quantum computation [105]. The most common approach to create cluster states in CV is the application of CZ gate in phase quadrature eigenstates $|p\rangle = 0$, along the qumodes square lattice [56]. In CV analog of qubit cluster states $|+\rangle$ becomes $|0\rangle_p$. The Z measurements are replaced by $\hat{q}$, and X measurements are replaced by $\hat{p}$. The CV analog of qubit controlled phase gate is $CZ = e^{i\hat{q}_i\hat{q}_j}$, used for entangling the nodes i and j.

Equation (4) illustrates a two-qubit cluster state, while (5) illustrates the qumode counterpart.

$$C_z |+\rangle_1 |+\rangle_2 = |0\rangle_1 |0\rangle_2 + |0\rangle_1 |1\rangle_2 + |0\rangle_1 |1\rangle_2 - |1\rangle_1 |1\rangle_2 \quad (4)$$

$$e^{i\alpha Q_1 Q_2} |p=0\rangle_1 |p'=0\rangle_2 = \frac{1}{2\pi} \iint dq dq' e^{i\alpha q_1 q_2} |q\rangle_1 |q'\rangle_2 \quad (5)$$

Such a cluster state in CV cannot be realized physically since they are infinitely squeezed, and practically only finitely phase-squeezed states can be physically implemented. To create these states, the degenerate optical parametric amplifiers (OPA), also known as single-mode squeezers are used, where quantum non-demolition operation is applied [106], [107], [108], which can also be called as controlled phase operation.

d: STABILIZER FORMALISM

Stabilizer formalism for CV systems, also known as nullifiers, [109], [110] can completely specify the CV based graph states [111], just like in the case of qubit cluster states. For instance, $X(s)$ is $+1$-eigenstate of momentum operator, it can stabilize the zero-momentum state $|0\rangle_p$. The stabilizers can be generalized for any CV based graph state $|\varphi\rangle$, with n modes and graph represented as $G = (V, E)$. Furthermore, EPR entangled states are the joint eigen states of two-mode commuting quantum variables [112] used in quantum optics as described in (6) and (7) ($P1+P2$ and $Q1-Q2$). The plus and minus signs can be interchanged, which means that quantum standard deviation and noise measurement for these operators will be zero ($\Delta(Q1 - Q2) = 0$ and $\Delta(P1 + P2) = 0$). These EPR operators are also known as nullifiers or variance-based entanglement witness, in CV-based quantum computation [56], and is used widely for entanglement verification in CV based cluster states.

$$P = \frac{1}{i\sqrt{2}}(a - a^\dagger) \quad (6)$$

$$Q = \frac{1}{i\sqrt{2}}(a + a^\dagger) \quad (7)$$

e: OPTICAL IMPLEMENTATION

Quantum optics is the most natural platform for the implementation of CV-based quantum computation using EPR entanglement [113], which is believed to be the most versatile entanglement resource for various QIP protocols [3], [94], with various applications, including quantum dense coding [114], quantum key distribution [115], unconditional quantum teleportation [116] and quantum secret sharing [117]. Moreover, implementing CNOT (a universal quantum gate) was demonstrated on quantum optics [118]. In quantum optical implementations of CV-based quantum computation, the amplitude and phase quadrature operators of quantum electromagnetic field, as shown in Equation (6) and (7), are the primary quantum variables for the underlying quantum computation [56], and are the mathematical equivalent of momentum and position operators of quantum harmonic oscillator of annihilation operator. The term quadrature encapsulates the free evolution of harmonic oscillator's momentum and position. The corresponding quantum gates and operations in CV-based quantum computation to that of qubit-based quantum computation are presented in a recent survey [56].

f: INSEPARABILITY CRITERIA IN CV CLUSTER STATES

The state nullifiers as discussed above in this section are linear combinations of momentum and position operartors for which the cluster states are eigenstates with 0 eigenvalue. The uncertainty measurement of the state nullifiers typically determines the inseparability in multi-partite cluster states [78]. However, when it comes to actual experimental realization, the cluster states do not behave as exact eigenstates of nullifiers, and measurement results in uncertainties around zero. According to van Loock-Furusawa criteria of inseparability [119], two or more sets of modes for a given cluster state are formed and an inequality is then derived with combined quadrature variance (usually should be <-3dB for linear CV cluster states). Any violation in that inequality results in failure of inseparability criteria for the underlying cluster state, and might result in failure of entanglement detection - an imperative feature of cluster states. Hence, the initial degree of quadrature squeezing directly effects the entanglement of quantum oscillator being exploited to make cluster state. Among others, a relatively recent work [76], highlights the minimum squeezing criteria for cluster state generation.

g: SCALABILITY OF CV CLUSTER STATES

Scalability is at the heart of universal quantum computation. From the scalability viewpoint of canonical method of cluster states generation in CV domain, N number of degenerate OPAs are needed for an N-mode cluster state with approximately two online OPAs (squeezers), for a single entangling operation [75]. This approach is often termed "bottom up" approach in the literature. The experimental resources increase linearly with the size of cluster state to be created and hence not very scalable [56]. After the realization of the fact that any N-mode graph state with arbitrary accuracy s, is a multi-mode Gaussian resource [75], [110], the canonical cluster state creation protocol can be recast as a Bloch-Messiah Reduction (BMR) [75]. The BMR approach allows to decompose a complex Gaussian unitary into simple scheme, where linear optical components can be separated from non-linear components. The cluster state creation approach, by exploiting the BMR technique, is usually termed as decomposition or top-down approach. The decomposition approach removes the requirement of two online squeezers for entangling operation in canonical approach of cluster state creation by sandwiching an N-single mode OPAs between the two N-mode interferometers [120]. The cluster state can then be created with offline squeezing (vacuum state squeezing) and linear optics, which in fact is

more advantageous since the online squeezing (squeezing of an arbitrary state of electromagnetic field) is experimentally more challenging than offline. The first interferometer becomes irrelevant in case of vacuum states as input states and a single N-mode interferometer can effectively realize such Gaussian states, which significantly simplifies the cluster state creation protocol by using the linear optical interferometer instead of optical controlled phase gates [110], [121]. Furthermore, it has been proved in [78], that offline squeezing saves significant amount of dBs as compared to online squeezing and hence increasing the number of qumodes being generated.

As discussed, the entangling operation's requirement of two OPAs has already been solved via the top-down approach, however the use of N number of OPOs for scaling up to N-mode cluster state is still a major hurdle in the context of experimental realization of CV-based cluster states, constraining the scalability of CV cluster states. Another improvement on scaling CV-based cluster states is the idea of using the whole quantum optical frequency comb (QOFC) of a single OPO for scaling up to N-mode CV cluster state rather than using N number of OPO's for scaling up to N-mode CV cluster state [56]. Moreover, the idea of using whole QOFC of single OPO also surpassed the requirement of interferometers, and hence providing a great potential for scaling the cluster states [92]. The first implementation exploiting the N-mode squeezing for the generation of N-mode entanglement was only for the GHZ state [91], which was then extended to cluster state generation [122], with square lattice configuration using a single OPO [92].

A. EXPERIMENTAL REALIZATION OF CV CLUSTER STATES

Quantum optics provides a scalable platform for universal CV-based quantum computation. This has been demonstrated with frequency and temporal phase-locked quantum optical combs, which are emitted by OPOs [56], [73], [92], [123]. Moreover, it has been shown in [105], that cluster states are generated upon interference of shifted, two-mode-squeezed optical combs. These states are the universal resources for quantum computation [37], in time and frequency domains, discussed later in this section. The two-mode-squeezing states, sometimes known as EPR pairs, are the building blocks of a CV cluster state [56]. Entangling qumodes from different EPR pairs results in cluster state chain, also called quantum wire. Recently, the optical spatial comb has also been used to realize CV cluster states using spatial multiplexing, also discussed later in this section. In the following subsections, we will discuss state-of-the art CV cluster states using temporal, frequency and spatial domains. Furthermore, hybrid approaches, using a combination of any two of the multiplexing approaches, are also discussed.

1) USING FREQUENCY DOMAIN MULTIPLEXING

In frequency domain realization of CV cluster states, the entangled modes are simultaneously generated [96]. In frequency domain the input EPR pairs straddle many frequencies and two orthogonal polarizations, created in two sets at two orthogonal linear polarizations. The pairs at one polarization are shifted with respect to the pair at another polarization by frequency shifting of the independent pump fields that creates each pair set, Fig. 5a. This frequency shifting is a lossless operation. All EPR pairs are emitted in the same cavity mode and are subjected to balanced beam splitting by undergoing a 45° polarization rotation in a halfwave plate resulting in a dual-rail quantum wire, as shown in Fig. 5b.

A prominent advantage of frequency domain is the lossless implementation of large delays, which are needed for scaling up to large number of wires, as compared to implementation in time domain where optical fiber delay lines are usually used. However, the frequency domain implementation is limited by the phasematching bandwidth whereas time domain implementation is limited by characteristic stability time of experiment under consideration, which has no fundamental restriction [56].

A limitation of frequency domain is the possibility of running out of the phasematching bandwidth due to OPO crystals dispersion. In such a case the QOFC's FSR's become chirped and qumodes which are far away from the pump's half-frequency will shift out of OPO resonance [56]. A proper use of spectrally broadened pump field can help overcoming this very problem [97].

Some initial proposals for the generation of cluster states based on continuous variables using frequency domain multiplexing [73], [85], involved the use of online squeezers (seeded OPOs [92]), which are quite challenging to implement. However, as discussed earlier in section V-0.c, a more practical approach is the use of Bloch-Messiah decomposition, which makes use of N number of vacuum squeezers along with $\mathcal{O}(N^2)$ port interferrometers [110]. This very method also uses significant number of experimental resources and hence offer limited scalability. To overcome this issue in terms of scalability of CV-based cluster states, a new approach for the creation of larger cluster states, having a compact experimental setup is proposed in [92], and is also called top-down approach. This approach offers a promising scaling potential since it only uses a single OPO and no interferrometer.

The initial proposal on square-lattice cluster state creation exploiting a single OPO was presented in [92] and [123] and is shown in Fig. 6, which overcame the no-go theorem in linear chain and square lattice cluster states creation using QOFC [123]. The proposal expanded the proof (cluster states creation using single OPO by using its whole QOFC), by the addition of an extra degree of freedom (polarization) to the qumode's frequency labels. A doubly resonant OPO containing a periodically poled KTiOPO4 (KTP) crystal with phase matching the three different pump/signal/signal polarization sets ZZZ, ZYY and YZY/YYZ, all with same coupling strengths was used for the implementation of polarization block. The experimental demonstration of this crystal is presented in [124].

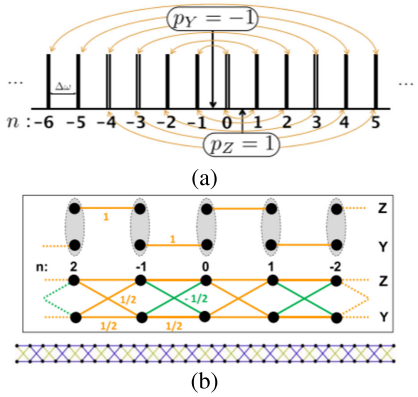

FIGURE 5. Generation of CV Dual-rail Quantum wire in Frequency Domain [96]: (a) Initial graph in quantum optical frequency comb. The arrow indicates pumps' half frequencies. (b) A chain structure is formed by the recorded frequencies. The ovals represent the balanced beam splitter interactions. The measured 60 qumode CV cluster state is at the right panel of (b).

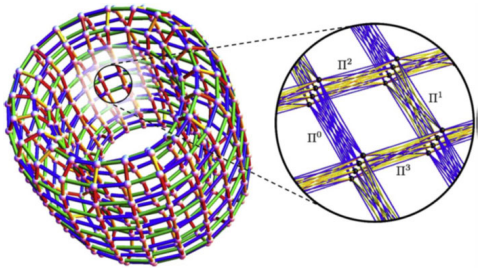

FIGURE 6. Toroidal cluster state generation in Square lattice configuration [92]. (Left): The resulting graph for CV cluster state. (Right): each white vertex comprises of a set of four individual qumodes which are labelled by two orthogonal polarization and two frequencies. The non-linear interactions (ZYY,ZZZ and YZY/YYZ) are represented by blue and yellow edges respectively.

The non-trivial frequency spacing and a fairly complicated 15-mode pump field with orthogonal ±45° polarization components is slightly inconvenient in this proposal, which needs sophisticated phase modulation techniques for producing the single side bands [125] at multiple frequencies. This inconvenience led to the exploration of other techniques for cluster state generation, it is still, however compact and might be implementable in future.

An experimental implementation of proposal [126], for multiple 2×2 cluster state creation is presented in [95]. Despite having smaller cluster size, it exhibits a great scalability potential because of the simultaneous generation of 15 copies of square lattices with each having 4 qumodes and hence a total of 60 qumodes cluster state. However, the limited number of qumodes in the resulting state are primarily due to the experimental limitations and more sophisticated setup would lead to at least three times larger cluster state [95]. This was the first large scale cluster state generation. The OPO has two KTP crystals where one was phase-matched the ZZZ and YZY/YZ interactions simultaneously and is coupled with two frequencies and two polarizations with a single pump frequency.

While using the QOFC, the scalability of a cluster state is not only dependent on the number of qumodes (state size) but also on the number of copies of the state [56]. To see this in frequency domain (Fig. 5a), we detune the pump half-frequencies by an integer multiple of the OPO FSR. This idea has been demonstrated in [96], where, by using a single OPO result in two independent quantum wires each having 30 qumodes. The same proposal also implements a single dial-rail quantum wire with simultaneously accessible 60 qumodes (Fig. 5).

An $N \times N$ square lattice in frequency domain is proposed in [98], where two QOFC's were interfered. One QOFC was hosting half pump detuning of 1 FSR (single wire whereas the other QOFC was hosting the half pump detuning of N FSRs (N independent wires). This proposal was based on the original temporal idea of [127], but it opened doors to new type of scalability where, by using only one QOFC per dimension and generalized interferometers in a fractal procedure [98], we can go from 1D to 2D and then 2D to 4D.

Most of the above-mentioned proposals depend on the interference of two to four squeezed quantum frequency combs. Recently, a frequency domain realization of CV cluster states with more compact experimental configuration was proposed [120], where only a single comb is shown to be sufficient for the generation of n-hypercubic cluster states having arbitrary dimension n. Moreover, cluster states with 1D, 2D and 3D have also been realized. In [120], phase modulation via sparse discrete spectrum is performed on QOFC generated by a single OPO. The size of cluster state is dependent on the spacing between the modulation frequencies and the dimension of cluster state is determined by the total number of modulation frequencies. First, independent EPR qumodes pairs in TMS states, also known as EPR pairs, are generated over QOFC by a single doubly resonant OPO with a single pump frequency evenly distributed between two OPO mode frequencies following the procedure as in Fig. 5a. Second, by optical or RF means, phase modulation is performed at frequency multiple of comb spacing.

The entanglement is scalable in terms of number copies of bipartite EPR states, but not in terms of size of multipartite state. It was shown in [120] that performing phase modulation of the OPO's QOFC by an EOM in 1, 2 and 3 frequencies will lead to the creation of 1D, 2D and 3D cluster states. For 1D cluster states, single phase modulation with 0, 0.1, 0.2, 0.5 and 1 radian, with an initial squeezing parameter of 2.3 was performed resulting in different configuration of 1D dual-rail cluster states. A typical structure of generated 1D graph is shown in Fig. 7.

Phase modulation at an additional frequency in the setup from Fig. 7 yielded a 2D cluster state. The two phase modulation frequencies for 2D cluster states were $\Omega_1 = 1$, which created a ladder graph just like 1D case, and $\Omega_2 = 10$, which introduced additional coupling after every 10 modes, transforming the 1D graph to 2D, as shown in Fig. 8a.

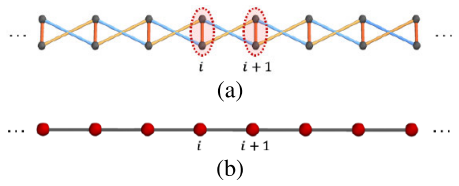

FIGURE 7. Generated 1D cluster state [120]. (a) the red ovals represents EPR- qumodes containg two modes. (b) Compact Graph representation of 1D cluster states using EPR macronodes.

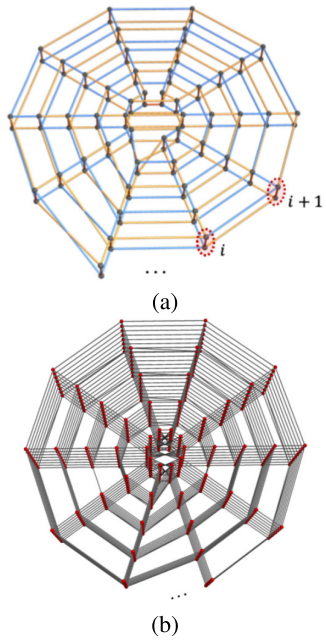

FIGURE 8. Generated 2D and 3D cluster states [120]. (a) the red ovals represent the EPR qumodes, each containing two modes with one mode in top layer and one in the bottom layer. (b) The generated 3D cluster state in cylindrical configuration.

The width of square lattice (number of spokes) in the 2D case is determined by Ω_2/Ω_1. The total number of qumodes generated is determined by phasematching bandwidth of the non-linear medium in OPO. Addition of another modulation frequency lead to 3D cluster state generation, Fig. 8b. The modulation frequencies for 3D cluster state were, $\Omega_1 = 1$, $\Omega_2 = 8$ and $\Omega_3 = 80$. The length of cylindrical cluster state is set by Ω_2/Ω_1 and number of spoke in 3D case are set by Ω_3/Ω_2. An increase in the number of modes increases the spoke radius as N/Ω_3. The example of generated 3D cluster state as shown in Fig. 8b, has 400 macronodes with 10 spokes, 5 set of macronodes in radial direction and a length of 8 macronodes. All state-of-the-art approaches exploiting frequency domain multiplexing for cluster states realization are summarized in Table 3.

2) USING TIME DOMAIN MULTIPLEXING

Another approach to realize CV cluster state is time domain multiplexing, which has seen considerable attention in the recent years. In time domain multiplexing, two-single mode squeezed states are interferred in quadrature to create spatially separated EPR pairs [56]. A dual rail quantum wire structure is created by passing one qumode of one of the EPR pair through delay line before its interference with a qumode of next EPR pair at a beam splitter. The experimental realization of this idea is presented in [85], with 10^4 qumodes in a single chain. This idea was later extended to generate around one million qumodes that are sequentially accessible (two qumodes can be accessed simultaneously [86]). It is important to note that even the sequential access of qumodes is compatible with quantum computation and is termed as the Wallace and Gromit approach [128].

The top-down and bottom-up approaches are also being used for cluster states realization in time domain. When using the whole QOFC of a single OPO while scaling the CV cluster state, the scalability is not only dependent on the number of modes per state (state size), but also on the number of copies of the state. For the realization of square or hypercubic cluster states in temporal domain, two commensurate delays are used to come up with a square lattice [56]. Although, such temporal delays pose a major limitation for the scalability of cluster states, the experimental implementation of cluster states using this approach has progressed well recently [78], [84].

A deterministic generation of continuous variable cluster state, called extended Einstein-Podolsky-Rosen (XEPR) state, along with its full characterization is presented in [85], which enables the ultra-large scale QIP based on MBQC, since the generated cluster state contains more than 10,000 entangled modes. These entangled modes are time domain multiplexed wave-packets of light. Combining two XEPR states with different time delays using additional beam splitters can help achieve universal MBQC [77]. The primary reason behind the creation of large number of entangled modes is that only a small subset of the whole XERP state exists at each instant of time in the time domain multiplexed demonstration. The sequentially propagating EPR states which are contained in two distinct beams were entangled for the generation of XEPR states.

Soon after the realization of XEPR cluster state containing 10,000 entangled modes, a CV-based cluster state with around one-million modes was developed [86]. The authors highlighted and addressed the issues in XEPR cluster state realization in [85], such as the the long optical delay line in the optical setup, and the noisy modulated bright beams used for phase locking (necessary for cluster state generation). These modulated beams treat interference signals as error signals for feedback control. All these issues lead to failure in inseparability criteria [119], after 16000 entangled modes in 1.3ms [85]. To overcome these issues, continuing feedback control strategy for the optical system was used in [86] during cluster state generation and electrically removing the noise of modulated bright beams helped in achieving more than one million entangled modes without any degradation in squeezing criteria. The inseparability criteria for enough entanglement witness between the qumodes is calculated to

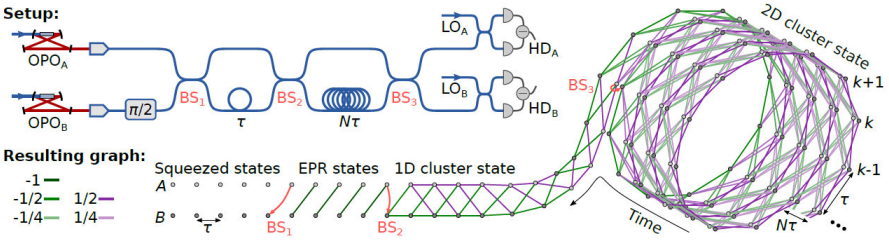

FIGURE 9. Generation Process of 2D cluster state [78]. The OPO_A and OPO_B produce squeezing. The EPR states are created by the interference of the temporal modes of squeezing with mode index k in two spatial modes A and B at beamsplitter (BS_1). The mode B is then delayed by τ and EPR pairs get entangled at beamsplitter (BS_2) to form a 1D cluster state. The mode B is again delayed by N_τ and the 1D cluster state is curled up to form a 2D cluster state at beamsplitter (BS_3). The homodyne detectors HD_A and HD_B are used for measuring the temporal mode quadratures which then aid towards nullifiers calculation.

be −3 dB. However, the qumodes up to 6×10^5 modes had nullifier variances well below the inseparability with $\hat{n}_k^p = -4.3 \pm 0.2\ dB$ and $\hat{n}_k^x = -4.3 \pm 0.2\ dB$. The worst variances reported for qumodes over 6×10^5 are $\hat{n}_k^p = -3.6\ dB$ and $\hat{n}_k^x = -3.5\ dB$.

The cluster states realizations discussed above are 1D and/or dual rail. However, for universal quantum computation, multi-qubit (or qumodes in CV case), operations are imperative, which usually needs cluster states having two or more dimensions [98], [127], [129]. A two-dimensional cluster state is usually a square lattice configuration of qumodes, which has been realized in CV using time domain multiplexing [78], [84]. The position and momentum quadrature's of photonic harmonic oscillator [93], were used for information encoding. A long chain of entangled modes were generated in Larsen:2019 by temporal multiplexing of optical Einstein-Podolsky-Rosen (EPR) states [130], which was then curled and fused into a two-dimensional (2D) cylindrical array of qumodes. An abstract experimental setup demonstration along with the generated cluster state is shown in Fig. 9.

A total of 30,000 entangled modes are generated in [78] with $2 \times 12 = 24$ modes as input registers (each having 1250 modes), which can be used for encoding the input state. The inseparability bound for entanglement creation between qumodes was found to be -3dB and is satisfied by the qumodes of generated cluster states, as presented in tabular summary at the end of this section. Furthermore, the proposed approach in [78] is quite flexible for upscaling mainly because of its deterministic generation and easy-to-achieve experimental conditions in optical fibers.

Another recent experimental implementation of large scale 2D CV cluster state is presented in [84], which is capable to implement universal MBQC in CV domain. The total number of qumodes generated are around 25000 with 5 input modes and a computation depth of 5000 modes. Multiple temporally localized square shaped cluster state on four beams which are spatially separated are used for generation of 2D CV time domain multiplexed cluster state by exploiting time domain multiplexing. Two optical delay lines are used for creating the 2D structure. The delay of an optical delay line is same as time interval between temporal modes of the state. The delay of other line is equal to the product of number of input modes for quantum computation and time interval between temporal modes. Finally, a 2D cluster state is created by first delaying the modes on two beams and then connecting them to temporal modes on two non-delayed beams. An example cluster state for 30 input modes is similar to that created for frequency domain multiplexing (Fig. 6). The inseparability criteria for the generated qumodes is found to be less than −4.5 dB and is fulfilled.

More recently, a novel approach for the generation of large-scale three-dimensional (3D) topological cluster state, was proposed in [131], providing a platform for topologically protected MBQC. The proposed approach combines the time domain multiplexing and divide-and-conquer approach [68], [132], resulting in two prominent advantages. Firstly, for entanglement verification of the created cluster state, the squeezing levels are quite feasible in terms of experimental implementation, because the squeezing level needed for the proposed 3D cluster state is ≃4.77dB, which does not exceed much from that of 2D cluster state exploiting only the time domain multiplexing, which is recently reported in [84] and is ≃4.5dB. Secondly, the generated cluster state exhibits promising robustness against analog errors. These two advantages make it an appropriate choice for large scale quantum computation in CV domain. All the state-of-the-art techniques using time domain multiplexing for cluster states generation are summarized in Table 2.

3) USING SPATIAL MULTIPLEXING

Analogous to exploitation of optical frequency comb in frequency domain multiplexing approaches for cluster states realization, the spatial mode multiplexing exploits the spatial mode comb, which is slightly different yet an effective approach for large-scale cluster states realization. The spatial freedom of light is quite effective for up scaling the number of entangled modes (cluster state) [133] and can bring new improvements and extensions in cluster states physical realization. Spatial multiplexing offers some advantages which can lead to large scale generation of cluster states. First and

TABLE 2. State-of-the-art cluster state realization using time domain multiplexing.

Ref #		[85]	[86]	[78]	[84]
Cluster state dimension		1D-dual rail	1D-dual rail	2D	2D
Computation depth		-	-	1250	5000
No.of qumodes		10,000	1.2×10^6	30,000	$\simeq$25,000
No.of squeezed light sources		2	2	2	4
No of beam splitters		2	2	3	5
No of optical delay lines		1	1	2	2
Qumodes inseparability bound		-3 dB	-3 dB	-3 dB	-4.5 dB
Multiplexing time		$157.5ns$	$160ns$	$371\mu s^*$ $371ms^{**}$	$200ns$
Nullifier variances	$\hat{n}_k^p$	-5.2 ± 0.2 dB	-4.3 ± 0.2dB[1]	-4.3dB* -4.4 dB**	-5.34 ± 0.06 dB† -4.3 ± 0.2dB††
	$\hat{n}_k^x$	-4.9 ± 0.2 dB	-4.3 ± 0.2 dB[1]	-4.3 dB* -4.4 dB**	-5.34 ± 0.06 dB† -4.3 ± 0.2 dB††
Output sampling rate		200 MHz	100 MHz	250 MHz	1 GHz

[1] $first 6 \times 10^5 qumodes$
* $SmallDataset(1500qumodes)$
** $LargeDataset(15000qumodes)$
† $Firstdelayline$
† † $Seconddelayline$

foremost, in frequency multiplexing the small interval of frequency comb is dependent on free spectral range (FSR) of optical cavity, which makes it experimentally quite challenging to spatially separate them, whereas spatial modulators can quite efficiently spatially separate the modes in case of spatial modes [134]. Moreover, as opposed to temporal and frequency modes where experimentally challenging local light fields with accurate frequency and more measurement times are prepared for modes detection, the detection of spatial modes is relatively simpler and can be detected by multi-quadrant detectors [134]. Spatial multimode entanglement has already been explored in [135] and [136] by exploiting a single multimode OPA with the generation of spatial quadripartite GHZ entanglement [133] and CV hyper entanglement in [80] and [136].

As discussed, multiplexing in time or frequency domain are widely used for CV cluster states realization. The multiplexing is performed in OPOs both below and above threshold. A combination of entangling operators and beam splitter transformations governs the cluster states realization in these approaches. A similar transformation exists for OPAs with Gaussian input states that are operating on multiple spatial modes, where a careful selection of local oscillators leads to spatial mode distribution similar to that of optical frequency comb having axial modes in OPO cavity [137], which can then be exploited for cluster states generation.

The first ever theoretical proposal to use multi-spatial mode amplifier configuration capable of generating dual-rail cluster states over optical spatial comb was proposed in 2014 in [137]. That scheme uses insensitive amplifiers with concurrent phase based on four-wave mixing in alkali metals vapors. Every concurrent amplifier operates on independent spatial modes. A careful selection of local oscillator for entangled spatial modes measurement then helped to generate a spatial frequency comb from amplified spatial modes. These spatial modes are then mixed via linear transformation for the generation of the cluster state. The primary focus in [137] was to develop an analogy between optical frequency comb and optical spatial mode comb, which was then used for a dual rail cluster state realization. The proposed setup can be used to generate and detect cluster states using images to synthesize appropriate local oscillators. The proposed setup offers various advantages, such as ease of alignment, simple phase control and scalability using multiple gain regions. However, a potential disadvantage for that scheme is any local oscillator's misalignment can introduce noise due to the use of multiple OPOs rather than a single OPO.

In 2016, an experimental scheme for the generation of cluster states based on spatial mode combs by using a large-Fresnel-number degenerate optical parametric oscillator (DOPO) was proposed in [87]. An eleven-partite dual-rail cluster state was generated, similar to what is depicted in Fig. 5. Two spatial Laguerre-Gaussian (LG) modes with the same frequency were used for DOPO pumping (lg_l^p). The non-linear crystal of type I-phase matching (χ^2) was used in the cavity assuring the sustainable and simultaneous non-linear interaction between all down-converted and pump modes.

In 2017, the same group of researchers who proposed [87], came up with a new scheme for generating large-scale CV-based dual rail cluster state with more than 20 qumodes, by using a specially designed self-imaging OPO [134]. The proposed scheme with special OPO design is capable of multiplying the number of qumodes. It exploits the spatial mode comb in a self-imaging OPO. Two spatial Laguerre-Gaussian modes with same frequency and different polarization are used for pumping the OPO. The experimental setup uses two polarized type-zero phase matching nonlinear crystals are placed within four-mirror ring cavity and EPR pairs are generated using PDC, which were then concatenated and in turn extends to optical spatial mode comb and are connected by curved arrows, similar to Fig. 5a. This optical spatial mode

comb is then passed from a single beam splitter resulting in a large scale dual-rail cluster state, in a similar way as the one illustrated in Fig. 5b. The Van Loock Fursawa criteria of qumodes' full inseparability [119], is used for the evaluation of entanglement and it is shown that entanglement exists over a vast range of pump parameter and analyzing frequency.

The entanglement between co-propagating modes in one beam using spatial domain has previously been demonstrated in [138]. The cluster state was also created where qumodes are defined as combinations of different spatial regions of one beam [139]. More recently, in 2018, a CV square cluster state was developed by multiplexing the orthogonal spatial modes in single OPO [140]. Moreover, the pump profile is optimized by separately controlling the temperature of nonlinear crystals inside the OPA cavity, during the experiment, which significantly improved the entanglement quality. Two first order Hermite-Gauss (HG) modes with one beam in a single multi-mode OPA is used for creating the multimode entanglement, which is then transformed into a cluster state by phase correction. This approach is scalable for multimode entanglement in spatial domain, and eventually to spatial cluster states, which are basic resource for spatial quantum information processing. The total efficiency of the experimentation process is determined by product of propagation efficiency ($n_{prop} = 0.96 \pm 0.02$ dB), photodiode efficiency ($n_{phot} = 0.92 \pm 0.02$ dB) and the efficiency of spatial overlap in the homodyne detector ($n_{hd} = 0.96 \pm 0.02$ dB).

All the state-of-the-art approaches exploiting spatial domain multiplexing for cluster states realization are summarized in Table 3.

4) HYBRID APPROACHES

All the previous techniques, alone, can be visualized as 1D set of entangled modes; for instance, frequency and time domain multiplexing [79] as shown in Fig. 10a. Although these approaches, single handedly can increase the number of qumodes and eventually the available information in an optical channel, a combination of these approaches can optimize channel capacity and hence provide more information by exploiting all the available encoding space [79]; Fig. 10b.

Although, exploitation of these multiplexing techniques alone led to the creation of significantly large cluster states, a fully scalable experimental demonstration for 1WQC is still an open research problem. For that purpose, a combination of these approaches (temporal, frequency and spatial) is being used in order to obtain the best possible results. We now give an overview of some of the recent hybrid approached for CV cluster state realization.

One of the earliest proposal using a combination of time and frequency domain multiplexing, based on quantum memories is presented in 2014 in [79], for the cluster state generation. However, this approach follows the canonical method of CV cluster state generation (implementation of controlled-phase (CZ) gate for introducing the entanglement between generated qumodes) and is therefore not very scalable since

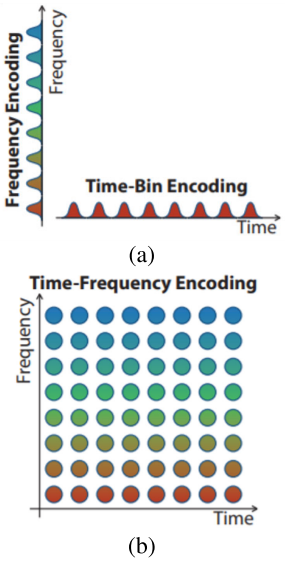

FIGURE 10. Time, Frequency and Hybrid (Time and Frequency) encoding [79]: (a) Separate frequency modes and time-bin modes encoding of quantum information (b) Combined time and frequency encoding leading to a maximum channel capacity (qumodes) and eventually more quantum information.

CZ gate implementation in quantum optics is experimentally demanding.

Later in 2016, with independent developments in time and frequency domain CV cluster states realization, a hybrid approach combining frequency quantum wire generation from [96] and temporal entanglement from [127], was proposed [88], where a cluster state is created by entangling the quantum frequency comb of EPR pairs by a single OPO, both in frequency and temporal domain. The resulting lattice could potentially contain infinite number of modes in one dimension (temporal modes), based on [85] and up to 3×10^3 modes in the other dimension (frequency), based on [96]. Unlike previous proposal [79], where the use of CZ gate was an integral part of cluster state creation, here the cluster state creation follows a macronode approach [123], which is entangled into a bilayer square lattice (BSL), comprising of two qumodes per layer. In the hybrid proposal [88], the frequency domain quantum wires are exposed to temporal delays and beam splitting, which results in cluster states having square lattice configuration in both time and frequency domains. This square lattice of temporal beam splitter is applied to every other frequency modes. A properly unbalanced Mach-Zehnder interferometer can easily separate the even and odd frequencies in quantum domain [141]. In addition to the proposal, CV-based quantum computation is studied in detail to prove that such states are universal resources for universal MBQC [141].

Although proposals for large scale CV cluster states have already been demonstrated, especially in time domain multiplexing as discussed in Section V-A2, most of them are for 1D cluster states, which are not sufficient for universal 1WQC. Recently, 2D CV cluster states multiplexed in time

domain are also proposed [78], [84], but are limited by the number of accessible qumodes in one of the dimensions (not uniform dimensions). Furthermore, extending to two dimensions introduces additional losses, which affects scalability beyond 1D in time domain multiplexing. Hybrid approaches (multiplexed in both temporal and frequency approaches), as discussed above, increase the size of smaller dimension significantly, but obtaining the phase reference for the simultaneous access of all frequency modes is still an open research problem.

Keeping in mind the issues above, recently, in 2020, a hybrid approach exploiting the third-order Kerr nonlinearity multiplexed in both time and frequency domain to create reconfigurable cluster states of one, two and three dimensions, is proposed in [142]. Time domain multiplexing provides sequential access for unlimited number of modes, whereas frequency domain multiplexing allows a simultaneous access to hundreds of highly connected modes. Obtaining phase references to simultaneously access all the frequency modes, which was a key challenge in the previous proposal, can be resolved by the third-order Kerr nonlinearity since it can create a frequency comb soliton, which can then act as phase reference, providing a simultaneous access to large number of frequency modes and hence can be scaled to 3D structure without introducing any additional losses. A microring resonator (MR) is used for generating classical frequency comb reference and eventually large-scale cluster states. Four wave mixing (FWM) approach is used for creating the side bands. The process of creating the cluster states of different dimensions includes sending a continuous wave pump field having a power below than parametric oscillation threshold. The resonator is pumped at even frequencies whereas the output field modes are detected only at odd frequencies. Pairwise sidebands are created by coupling the FWM process with different cavity frequency modes. In [142], TMS states (0D cluster states) are created, which are then combined by 50:50 beam splitter to produce 1D cluster states or dual-rail quantum wire.

For the generation of 2D CV cluster state in [142], the 1D cluster state is extended by adding an unbalanced Mach-Zehnder interferometer (UMZI), a 50:50 integrated beam splitter and a delay line. This approach is quite similar to that one proposed in [73], for a 2D cluster state creation in time-frequency domain. However, a prominent advantage of this approach is an easier and more convenient integration on a photonic chip because of the shorter delay line, due to the larger bandwidth of MR.

For 3D CV cluster states generation in [142], the 2D cluster state setup were used with some modifications. Two copies of 2D cluster state generation setup were used but here balanced Mach-Zehnder interferometers (BMZIs) replaces the 50:50 integrated beam splitters, primarily because they can be tuned to work like 50:50 IBS and in such a way that CV cluster states can be created on the same chip.

Another hybrid approach for creating multipartite entangled states, this time using both frequency and spatial modes of an OPO is proposed recently in [143]. The proposed scheme can generate several cluster states in parallel. Moreover, the effect of finite squeezing on measurement of weighted graph states (graph states in CV domain can have weighted edges unlike qubit cluster states) is also discussed along with an illustration of the proposed approach for cluster states of 8 (Fig. 11), and 60 qumodes. In the experimental setup, two Laguerre-Gaussian (LG) pumps are used to pump the optical parametric amplification in a single OPO resulting in parallel creation of entangled modes in both spatial and frequency domains.

All the state-of-the-art hybrid approaches for cluster states realization are summarized in Table 3.

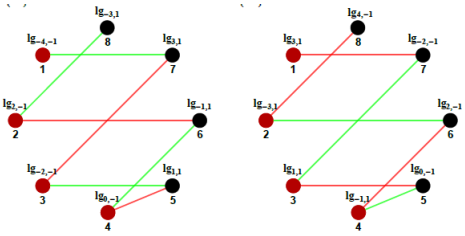

FIGURE 11. Two possible graph representations of an eight-mode cluster state [143]. Black and blue lines indicate two different pumps).

VI. DV-BASED QUANTUM COMPUTATION

DV-based computation is the standard and original approach to perform quantum computation using discrete observables rather than continuous ones; that is, qubits rather than qumodes. More details on DV based quantum computation, particularly in comparison to CV based quantum computation, can be found in [144].

A. EXPERIMENTAL REALIZATION OF DV CLUSTER STATES

Creating cluster states entails carefully entangling the underlying qubits. The cluster states in DV can be experimentally prepared by two methods: cooling the nearest-neighbor Ising-type Hamiltonian systems to its ground state or by dynamic implementation of CZ gates on a qubit lattice which are initialized in a superposition state $|+\rangle$, but measuring entanglement is non-trivial. Since the 1989 discussion on entanglement of various mixed states by Werner [145], many criteria for entanglement measurement have been proposed. However, symmetric extension criteria [146] and partial transpose criteria [147], [148], [149] are the most widely used ones.

The photonic realization of cluster states focuses on the use of photons as potential qubits in a large cluster state, and are probabilistic as the cluster generation happens only upon the successful creation and detection of photons. Moreover, the quantum computation based on cluster states created by photons prepares the usual input states in $|+\rangle$ as part of initial cluster states. These attributes of DV-based cluster state generation limits their use whenever there is a need of deterministic application of unitary gates on an input state which is not prepared in the cluster state (output of previous

computation) [150]. A number of research efforts have been made for realization of photonic cluster state enabling MBQC in photonic qubits. This section will summarize the proposals on photonic cluster states in MBQC context.

In [151], four photons were polarized to realize a four-qubit cluster state. Quantum state tomography [152] was used for the extraction of density matrix of a quantum state. The cluster state fidelity of 0.60 ± 0.02 was achieved surpassing the local realism threshold of 0.56. Arbitrary single qubit rotations SU(2) and two qubit operations (CPhase and CNOT) were implemented with an average fidelity rate of 0.85 ± 0.04. and 0.93 ± 0.01 respectively. Grover's search algorithm [7] with success probability of 90% was also implemented.

Another proof-of-principle demonstration of 1WQC was presented in [45], where a two-photon four-qubit cluster state resource is developed and is entangled in both spatial and polarization modes of photons, with a state fidelity rate exceeding 88%. Afterwards, two-qubit quantum gates were implemented with around 95% average fidelity rates and grover algorithm with success probability of around 96%.

In [48], a four-qubit cluster state with fidelity rate of 0.880 ± 0.013 was realized by exploiting the full entanglement of two photons having two degrees of freedom (linear momentum and polarization). Arbitrary single qubit rotations and two qubit operations (CNOT and CPhase) gates were implemented with average fidelity rates of 0.867 ± 0.018 and 0.907 ± 0.010 respectively.

Hyperentanglement [153] has been used widely to increase the number of qubits without increasing the photons. In this approach, the particles (photons) are entangled in various degrees of freedom [45], [154], [155], [156], which can potentially increase fidelity and qubit generation rate. Since 1WQC requires high number of qubits to create cluster state [157] hyperentanglement is very well suited for it's physical realization. Based on same approach, a two-photon six-qubit linear cluster state was developed in [158], where each particle encodes three qubits exploiting two distinct degrees of freedom of photons. Linear momentum encodes two qubits whereas a single qubit is encoded in photon polariztion. The cluster state fidelity of 0.6350 ± 0.0008 was achieved, better than the previously proposed six-qubit cluster states. In a similar fashion, four photons were used to develop a six-qubit cluster state in [157]. The photons were entangled in polarization and spatial modes. The overall cluster state fidelity achieved was $0.61 \pm 0.01\%$ and a CNOT gate with fidelity rate of $79 \pm 1\%$ was also implemented using the created cluster state.

In [159], four photons in horizontal polarization were used to develop a four-qubit cluster state. The average cluster state fidelity of 0.860 ± 0.015 was achieved. Furthermore, arbitrary single qubit rotations were also implemented exploiting the created cluster state with an average fidelity rate of 0.926 ± 0.10. The fusion of path qubits is also one of the techniques to create cluster states with larger number of qubits with relatively lesser particles. In [51], a seven-qubit entangled cluster state was created by fusing two distinct two-photon four qubit linear graph states with an average fidelity rate of $>64\%$. To demonstrate the authenticity of developed cluster state two-bit Deutsch-Jozsa [9] algorithm was implemented with success probability of $>90\%$.

In [160], a high-brightness photonic crystal fiber (PCF) is used as an entangled photon pairs source [50], [161] to create a four-photon state by using a post selected fusion gate. A scalable formation of larger cluster states can be achieved using fusion gates. The term scalable here refers to begin with smaller entangled states source (Bell states) [162], [163] and going up to larger states. The fused four-photon cluster state has fidelity rate of 0.66 ± 0.01 was achieved. Single-qubit (Hadamard) gate was implemented with fidelity rate of 0.67 ± 0.03. Moroever, two-qubit (CNOT) gate and three-qubit (Toffoli) gate were implemented with fidelity rate of 0.64 ± 0.01 and 0.76 ± 0.04 respectively. The state-of-the-art photonic cluster states realization are summarized in Table 4.

The core of cluster states is entanglement, which might be challenging to create and maintain. In the following sub-sections, some recent proposals on qubits entanglement primarily in photonic and superconducting qubits, which potentially can be used as cluster state for MBQC, are discussed.

1) ENTANGLEMENT IN PHOTONIC QUBITS

Photonic qubits have the potential to be the future of QIP because of the advantages they offer over other candidates, such as improved speed, larger bandwidth, compatibility with CMOS fabrication, and most importantly improved decoherence, particularly for single photons. Hence, single photons are widely used for the realization of high precision quantum gates and cluster states realization on MBQC.

The first experimental demonstration of three spatially separated photons was proposed in [164]. Since then, multiple efforts have been made for entangling various number of qubits [165], [166], [167], [168], [169], [170], most of them are based on spontaneous parametric down conversion (SPDC) [171]. In 2012, a total of eight individual photons were successfully entangled [172] using an ultra-bright sources of entangled photon pairs [173] along with an eight-photon interferometer and post-selection detection. A total of four photon pairs were used in [172] which were then, by appropriate experimental setup, transformed to eight-photon GHZ state, with state fidelity of about 0.708 ± 0.016, which is greater than 0.5 threshold assuring the genuine multi-partite entanglement [174].

Later in 2016, an approach to entangle 10 spatially separated entangled single photons was proposed in [175]. The resulting state has the fidelity of about 0.57 greater than the genuine multi-partite entanglement threshold and hence confirming the genuine multi-partite entanglement between all the photonic qubits. The key factors in achieving 10-photon entanglement include SPDC photon pair source with high

TABLE 3. Summary of state-of-the-art cluster states in CV domain.

Ref#	Frequency Multiplexing	Time Multiplexing	Spatial Multiplexing	Cluster state dimension	No. of entangled modes
[95]	✓	–	–	2D	60*
[96]	✓	–	–	1D-dual rail	60
[98]	✓	–	–	1D,2D,3D	10^4
[120]	✓	–	–	1D,2D,3D,nD	10^4
[85]	–	✓	–	1D-dual rail	$10,000$
[86]	–	✓	–	1D-dual rail	1.2×10^6
[78]	–	✓	–	2D	$30,000$
[84]	–	✓	–	2D	25000
[137]	–	–	✓	1D-dual rail	$\simeq 200$
[87]	–	–	✓	1D	11-partite
[134]	–	–	✓	1D	>20
[140]	–	–	✓	2D	4
[79]	✓	✓	–	2D	–
[88]	✓	✓	–	2D	$3 \times 10^3 \times \infty$**
[142]	✓	✓	–	3D	>2000
[143]	✓	–	✓	–	$60^\dagger$

*15 copies of 2×2 cluster states
**3×10^3 modes in frequency domain and infinite modes in time domain
†FSR between 1-10GHz can generate up to $10^3 - 10^4$ modes

TABLE 4. State-of-the-art Cluster states in using discrete variables.

Ref#	Generated Cluster state	Implemented Algorithm	Cluster state fidelity	Average gate fidelity			Algorithm success
				Single qubit	Two qubit	Three qubit	
[151]	four-photon four-qubit	Grover's search algorithm	0.60 ± 0.02	0.85 ± 0.04	0.93 ± 0.01	–	0.90
[45]	Two-photon four-qubit	Grover's search algorithm	> 0.88	–	0.95	–	0.96
[51]	Seven-qubit	Deutsch-Jozsa algorithm	> 0.64	–	–	–	> 0.90
[48]	Two-photon four-qubit	–	0.880 ± 0.013	0.867 ± 0.018	0.907 ± 0.010	–	–
[158]	Two-photon six-qubit	–	0.635 ± 0.0008	–	–	–	–
[157]	Four-photon six-qubit	–	0.61 ± 0.01	–	79 ± 1	–	–
[159]	Four-photon Four-qubit	–	0.860 ± 0.010	0.926 ± 0.015	–	–	–
[160]	Four-photon	–	0.66 ± 0.01	0.67 ± 0.03	0.64 ± 0.01	0.76 ± 0.04	–

brightness, high collection efficiency and high photon indistinguishability.

In 2018, an experimental demonstration of 12-photon entanglement was proposed [176], by using an optimal SPDC entangled photon source with high indisguishability (96%), and efficiency (97%). The resulting state fidelity of 0.572 ± 0.024 was achieved ensuring genuine multi-partite entanglement between all the entangled qubits. In the same year, an experimental demonstration of entangling 18-qubit GHZ state was also proposed in [177] by exploiting three distinct degree of freedoms (polarization, spatial modes, and orbital angular momentum) of six photons. A genuine multipartite entanglement was confirmed between all 18 qubits with resulting state fidelity of 0.708 ± 0.016 which quite higher than 12-photon entanglement [176].

In all the proposals discussed above, probabilistic sources were used for entanglement creation which are restricted in terms of efficiency and high hardware cost. Recently, in 2020, a resource efficient sequential creation of linear cluster states from a single photon emitter was proposed [178]. A single entangling gate in a fiber loop configuration [179] was used for entangling the stream of incoming photonic qubits. A four-photon linear cluster state was generated; however the proposed setup is capable of creating a cluster state of arbitrary number of photons. Hence, the proposed approach exhibits tremendous scaling potential. The said

proposal makes use of semiconductor quantum dots for single photon creation sequentially [180], and temporal delay loop approach for entanglement generation [179]. The photon indistinguishability is measured at different time intervals and it ranges from 77% to 95%. Moreoevr, the genuine multi-partite entanglement has been verified in all four photons.

All the entanglement advances using photonic qubits are summarized in Table 5.

2) ENTANGLEMENT IN SUPERCONDUCTING QUBITS

Superconducting circuits are another promising approach for the realization of qubits and qubit gates. The advantages like scalablity, ability of easy coupling and control and high designability of superconducting circuits make them attractive for the physical realization of quantum computers [181]. Here, we report some recent proposals focusing on entangling the superconducting qubits which can potentially serve as resource states for MBQC.

In 2018, 16 superconducting qubits of IBM's quantum device ibmqx5 (16-qubit quantum device) were entangled using optimized low-depth circuits [182]. The graph states which are the generalization of cluster states [37], were used for entangling of the qubits. The starting point for graph state preparation was to build a circuit as per the definition of graph states (Section II-A). For entanglement between qubits CZ gates were implemented using one CNOT and two H-gates. which eventually produces between the qubits. The total of 5 graph states having ring configuration were created as shown in Fig. 12.

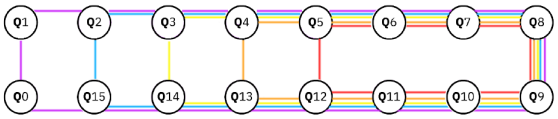

FIGURE 12. Graph states created in [182]. Red lines indicate the 8-qubit graph state, orange lines indicate the 10-qubit graph state and 12, 14 and 16-qubit graph states are represented by yellow, blue and purple lines respectively.

For entanglement detection in [182] reduced density matrices-based entanglement criterion up to 4 qubits (using maximum likelihood method [183]) was used and negativity of resulting two-qubit systems were calculated. All the negativity values for 8-qubit graph state were calculated to be significantly greater than zero and hence fully entangled. In case of 10-qubit graph state 9 out of 10 negativity values were greater than zero and is fully entangled, since it is claimed that for an n-qubit system if $n-1$ qubits are entangled then the whole system is entangled. For 12 and 14-qubit graph states, two of the negativities were calculated to be zero (not entangled), however with proper separation of qubits in these states and reduced density matrix calculations, it was proved that these states are also fully entangled. For a 16-qubit graph state 15 out of 16 negativities were greater than zero and hence fully entangled.

Another proposal entangling 20 qubits in a superconducting quantum computer was proposed recently in [184]. The entanglement was created on a 20 superconducting qubit IBM device (Poughkeepsie), and it was shown that all its 20 qubits can be entangled. A Graph state was prepared along the path of all 20 qubits following almost the same methodology as in [182]. The embedded graph state along with the entanglement between various qubits is shown in Fig. 13. Afterwards, full quantum state tomography was performed on every four connected qubits forming a chain along the path and negativity of every qubit pair was evaluated for entanglement detection. It was shown that every qubit pair is entangled leading to a conclusion that whole graph state is entangled and has better magnitue than [182]. Moreover, using entanglement witness it was shown that the chains of three qubits exhibits genuine multi-partite entanglement.

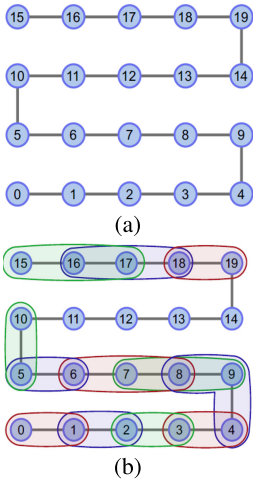

FIGURE 13. (a) Embedded Graph state on Poughkeepsie device where nodes represents qubits and edges represents two-qubit operations to create entanglement (b) Generated 20-qubit graph state highlighting regions of genuine multi-partite entanglement.

Recently in 2019, a genuine 12-qubit entanglement in linear configuration has been prepared and verified in a superconducting processor [185]. In this proposal the CZ gates are applied for the entanglement creation between the qubits in the processor. The superconducting processor used in the experiment consists of 12 transmon qubits [186], each having a fast flux-bias line (Z), a microwave drive line (XY) and a readout resonator. For the entanglement creation process, the qubits are initialized in state $|0\rangle$ and relaxed for 300μs. A total of 11 controlled phase (CZ) gates were used for entangling 12 qubits with fidelity of 0.5544 ± 0.0025.

In 2021, 27 superconducting qubits having the potential of being used as central resource for MBQC is proposed in [187]. The experiment was performed on ibmq_montreal device which comprises of 27 superconducting transmon qubits [186]. Alongside the entanglement, quantum read out

TABLE 5. Recent breakthroughs in qubits entanglement.

Ref #	Qubits type	No. of entangled qubits	Genuinely multi-partite entangled qubits	Resulting state fidelity
[172]	Photonic	8	all	0.708 ± 0.016
[175]	Photonic	10	all	0.573
[176]	Photonic	12	all	0.708 ± 0.016
[177]	Photonic	18	all	0.572 ± 0.024
[178]	Photonic	4*	all	–
[190]	Superconducting	20	18	0.5165 ± 0.0036
[185]	Superconducting	12	all	0.5544 ± 0.0025
[184]	Superconducting	20	all	–
[182]	Superconducting	16	all	–
[187]	Superconducting	26 27	all	0.62 ± 0.06 0.61 ± 0.05
[189]	Superconducting	53 65	all	–

* The proposed setup is capable to generate linear cluster having arbitrary number of photonic qubits

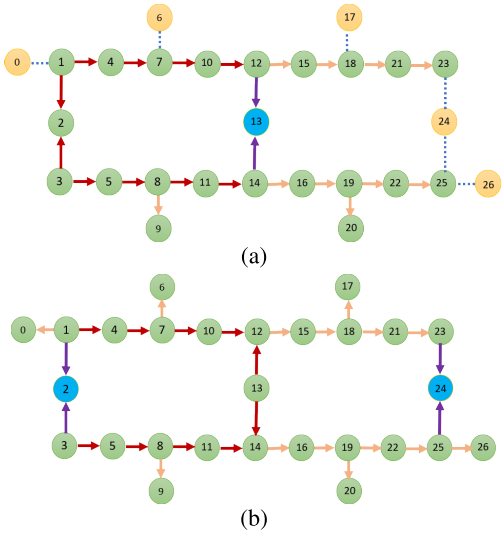

FIGURE 14. Created GHZ states on ibmq_montreal device [187]. The light green circles indicate qubits whereas light blue circles indicate the parity check qubits. The qubits not directly contributing to the experiment are represented by light orange circles. The arrows indicate the CNOT operation as: control_qubit→ target_qubit. The CNOT operations directly involved in GHZ state creation are represented by dark brown arrows. Light brown arrows represent CNOTs increasing the state size, purple arrows represent the CNOT operation involved in parity check. No two-qubit operation is applied on the qubits connected by dotted blue line.

error mitigation is also implemented [188], since the faulty measurements can affect the entanglement strength. Parity verification-a basic protocol for quantum error correction, was also investigated on resulting state fidelity. A total of two GHZ states (11-qubit state extended up to 19 qubits and 19-qubit state extended up to 25 qubits), were created with one and two parity check qubits respectively and are shown in Fig. 14. Additionally 26 and 27-qubit states were created with fidelity rates of 0.62 ± 0.06 and 0.61 ± 0.05 using quantum read out measurement, with genuine multi-partite entanglement across all the qubits.

Right after the 27-qubit entanglement on ibmq_montreal device [187], a largest till date, 53-qubit and 65-qubit IBM devices namely ibmq_rochester and ibmq_manhattan respectively, were entangled along with quantum read out measurements [189]. On 53-qubit ibmq_rochester device, without applying the quantum read out measurement technique resulting in entanglement of 31 out of 58 qubit pairs were entangled without applying the quantum read out measurement technique. The largest entangled region has maximum of 9 qubits. Similarly, 56 out of 58 qubit pairs were entangled with quantum read out measurement applied. The largest entangled region consists of all qubits of the device.

On ibmq_manhattan device, all the 72 qubit pairs were entangled in both cases (without applying the quantum read out measurement and with quantum read out measurement applied). Hence all 65 qubits of the device were successfully entangled. This is the largest qubit entanglement reported till date. The recent breakthroughs in qubit entanglement, which can potentially lead towards scalable MBQC are summarized in Table 5.

VII. CONCLUSION AND OUTLOOK

The race to achieve universal scalable quantum computation paradigm is in full swing over the last decade. MBQC is

one of the leading candidates exhibiting promising potential for scalable quantum computation. The computations in 1WQC completely relies on a highly entangled resource state (cluster state) and hence cluster states are integral part of 1WQC. Generation of such state, typically with higher dimensions (2D), already achieves universal quantum computation. Going beyond 2D, cluster states can potentially even achieve fault-tolerance. Over the last few years, development of these cluster states has attracted the research community, with two different main approaches: CV cluster states and DV cluster states. A CV cluster state is the combination of large number of entangled qumodes arranged in a cluster, whereas DV cluster state is the combination large number of qubits.

In this paper, we provide a comprehensive compilation and comparison of the techniques and approaches being used for cluster states realization in both CV and DV. While similar surveys exist [56], [57], these were not focused on the physical realization of MBQC.

CV cluster states can be realized on different approaches, namely: FDM, TDM, SDM and hybird. Among those, FDM and TDM are the most widely used ones. While FDM can generate cluster states with more than 3D dimensions, TDM can only generate 3D cluster states. Additionally, TDM can generate infinite number of qumodes, but allows only sequential access to qumodes, whereas FDM can generate sufficiently large number of qumodes while allowing simultaneous access them, which gives it slight edge over TDM. The SDM approach has also been explored with the largest cluster state dimension of 2D and limited number qumodes but still having the potential to scale up to large number of qubits and increased cluster state dimension. Recently, hybrid proposals for CV cluster state realization have been proposed using a combination of two multiplexing approaches. The largest hybrid CV cluster state of dimension up to 3D exploiting FDM and TDM has been reported in the literature. All the CV approaches are still in the developing and are equally likely to dominate in the future.

DV cluster states are based on qubits, and have been physically realized following different approaches, most notably: photons and superconducting circuits, where significant amount of research has been conducted already. These qubits can then be used to form the cluster states as required by MBQC. On photonic, large number photonic qubits have been successfully entangled, and research in this approach already looks promising. On superconducting, even larger number of qubits have been successful entangled, and research is progressing rapidly in this area.

Based on the surveyed literature, it seems that the CV track is currently leading the way towards scalable MBQC with cluster states dimensions of beyond 3D with thousands of entangled qumodes, whereas the largest number of entangled qubits reported in literature is 65. This smaller qubit number limitation is primarily due to the complex experimental procedure for qubits preparation and entanglement generation between them in DV. In summary, both CV and DV cluster state realizations are independently progressing at a rapid pace and it is hard to predict which approach could potentially be the future of scalable universal MBQC. The answer will not be straightforward, and may not even be either one, but (possibly) a combination.

Recently, entanglement generation by bridging both CV and DV approaches have been proposed in single hybrid experiments [144]. For example, an experimental illustration of teleporting DV qubits by using CV techniques has been presented in [191]. Entanglement generation between CV and DV qubits in [192] and [193] provided a foundation to communicate between DV and CV nodes and towards the realization of hybrid quantum networks. MBQC can also benefit from such hybrid approach where DV (non-Gaussian) projectors can be used to perform computations exploiting CV (Gaussian) cluster states [144]. Moreover, deterministic generation of multi-qubit gates in DV (particularly photonic) using MBQC is challenging as compared to CV and requires complex experimental setups. A combination of CV homodyne measurement and a relatively weak cross-Kerr nonlinearity can realize quantum non-demolition measurement making it possible to almost deterministically generate multi-qubit gate in DV with minimal experimental resources, which otherwise is extremely difficult [194]. To the best of our knowledge such approach is yet to be explored in the literature, adding one more direction for a potential fault-tolerate quantum computer based on MBQC.

ACKNOWLEDGMENT

The authors would like to thank the Qatar National Library for supporting the open access publication of this article.

REFERENCES

[1] B. J. Copeland, "The modern history of computing," in *The Stanford Encyclopedia of Philosophy*, E. N. Zalta, Ed. Stanford, CA, USA: Stanford Univ., Winter 2020.

[2] S. T. Marella and H. S. K. Parisa, "Introduction to quantum computing," in *Quantum Computing and Communications*. London, U.K.: IntechOpen, 2020.

[3] M. A. Nielsen, I. Chuang, and L. K. Grover, "Quantum computation and quantum information," *Amer. J. Phys.*, vol. 70, no. 5, pp. 558–559, May 2002.

[4] R. P. Feynman, "Simulating physics with computers," *Int. J. Theor. Phys.*, vol. 21, no. 6, pp. 467–488, 1982.

[5] F. Arute et al., "Quantum supremacy using a programmable superconducting processor," *Nature*, vol. 574, pp. 505–510, Oct. 2019.

[6] P. W. Shor, "Algorithms for quantum computation: Discrete logarithms and factoring," in *Proc. 35th Annu. Symp. Found. Comput. Sci.*, Nov. 1994, pp. 124–134.

[7] L. K. Grover, "A fast quantum mechanical algorithm for database search," in *Proc. 28th Annu. ACM Symp. Theory Comput. (STOC)*, 1996, pp. 212–219.

[8] E. Bernstein and U. Vazirani, "Quantum complexity theory," *SIAM J. Comput.*, vol. 26, no. 5, pp. 1411–1473, 1997.

[9] D. Deutsch and R. Jozsa, "Rapid solution of problems by quantum computation," *Proc. Roy. Soc. London A, Math. Phys. Sci.*, vol. 439, no. 1907, pp. 553–558, Dec. 1992.

[10] L. K. Grover, "A fast quantum mechanical algorithm for database search," in *Proc. 28th Annu. ACM Symp. Theory Comput. (STOC)*, Philadelphia, PA, USA. New York, NY, USA:Association for Computing Machinery, 1996, pp. 212–219, doi: 10.1145/237814.237866.

[11] H.-S. Zhong et al., "Quantum computational advantage using photons," *Science*, vol. 370, no. 6523, pp. 1460–1463, Dec. 2020.
[12] Y. Wu et al., "Strong quantum computational advantage using a superconducting quantum processor," *Phys. Rev. Lett.*, vol. 127, Oct. 2021, Art. no. 180501.
[13] C. C. McGeoch, *Adiabatic Quantum Computation and Quantum Annealing: Theory and Practice* (Synthesis Lectures on Quantum Computing), vol. 5, no. 2. Cham, Switzerland: Springer, Jul. 2014, pp. 1–93.
[14] I. S. Oliveira, T. J. Bonagamba, R. S. Sarthour, J. C. Freitas, and E. R. D. Azevedo, "Fundamentals of quantum computation and quantum information," in *NMR Quantum Information Processing*. Amsterdam, The Netherlands: Elsevier Science, 2007, pp. 93–136, ch. 3.
[15] R. Jozsa, "Entanglement and quantum computation," 1997, *arXiv:quant-ph/9707034*.
[16] T. Albash and D. A. Lidar, "Adiabatic quantum computation," *Rev. Mod. Phys.*, vol. 90, Jan. 2018, Art. no. 015002.
[17] S. Lloyd, M. Mohseni, and P. Rebentrost, "Quantum algorithms for supervised and unsupervised machine learning," 2013, *arXiv:1307.0411*.
[18] M. Benedetti, J. Realpe-Gómez, R. Biswas, and A. Perdomo-Ortiz, "Quantum-assisted learning of hardware-embedded probabilistic graphical models," *Phys. Rev. X*, vol. 7, no. 4, Nov. 2017, Art. no. 041052.
[19] R. Y. Li, R. D. Felice, R. Rohs, and D. A. Lidar, "Quantum annealing versus classical machine learning applied to a simplified computational biology problem," *npj Quantum Inf.*, vol. 4, no. 1, p. 14, Feb. 2018.
[20] H. Neven, V. S. Denchev, G. Rose, and W. G. Macready, "Training a large scale classifier with the quantum adiabatic algorithm," 2009, *arXiv:0912.0779*.
[21] A. Khoshaman, W. Vinci, B. Denis, E. Andriyash, H. Sadeghi, and M. H. Amin, "Quantum variational autoencoder," *Quantum Sci. Technol.*, vol. 4, no. 1, Sep. 2018, Art. no. 014001.
[22] M. Wilson, T. Vandal, T. Hogg, and E. G. Rieffel, "Quantum-assisted associative adversarial network: Applying quantum annealing in deep learning," *Quantum Mach. Intell.*, vol. 3, no. 1, p. 19, Jun. 2021.
[23] R. Ayanzadeh, S. Mousavi, M. Halem, and T. Finin, "Quantum annealing based binary compressive sensing with matrix uncertainty," 2019, *arXiv:1901.00088*.
[24] M. W. Johnson et al., "Quantum annealing with manufactured spins," *Nature*, vol. 473, pp. 194–198, May 2011.
[25] P. Hauke, H. G. Katzgraber, W. Lechner, H. Nishimori, and W. D. Oliver, "Perspectives of quantum annealing: Methods and implementations," *Rep. Prog. Phys.*, vol. 83, no. 5, May 2020, Art. no. 054401.
[26] M. Schuld, I. Sinayskiy, and F. Petruccione, "An introduction to quantum machine learning," *Contemp. Phys.*, vol. 56, pp. 172–185, Oct. 2014.
[27] J. Biamonte, P. Wittek, N. Pancotti, P. Rebentrost, N. Wiebe, and S. Lloyd, "Quantum machine learning," *Nature*, vol. 549, pp. 195–202, Sep. 2017.
[28] K. Beer, D. Bondarenko, T. Farrelly, T. J. Osborne, R. Salzmann, D. Scheiermann, and R. Wolf, "Training deep quantum neural networks," *Nature Commun.*, vol. 11, no. 1, pp. 1–6, Feb. 2020.
[29] M. Kashif and S. Al-Kuwari, "Design space exploration of hybrid quantum–classical neural networks," *Electronics*, vol. 10, no. 23, p. 2980, Nov. 2021.
[30] M. Kashif and S. Al-Kuwari, "The impact of cost function globality and locality in hybrid quantum neural networks on NISQ devices," *Mach. Learn., Sci. Technol.*, vol. 4, no. 1, Jan. 2023, Art. no. 015004.
[31] M. Kashif and S. Al-Kuwari, "Demonstrating quantum advantage in hybrid quantum neural networks for model capacity," in *Proc. IEEE Int. Conf. Rebooting Comput. (ICRC)*, Dec. 2022, pp. 36–44.
[32] M. Kashif and S. Al-kuwari, "ResQNets: A residual approach for mitigating barren plateaus in quantum neural networks," 2023, *arXiv:2305.03527*.
[33] M. Kashif and S. Al-Kuwari, "The unified effect of data encoding, ansatz expressibility and entanglement on the trainability of HQNNs," *Int. J. Parallel, Emergent Distrib. Syst.*, vol. 38, no. 5, pp. 362–400, 2023, doi: 10.1080/17445760.2023.2231163.
[34] B. E. Kane, "A silicon-based nuclear spin quantum computer," *Nature*, vol. 393, no. 6681, pp. 133–137, May 1998.
[35] D. Loss and D. P. DiVincenzo, "Quantum computation with quantum dots," *Phys. Rev. A, Gen. Phys.*, vol. 57, no. 1, pp. 120–126, Jan. 1998.
[36] S. C. Benjamin, B. W. Lovett, and J. M. Smith, "Prospects for measurement-based quantum computing with solid state spins," *Laser Photon. Rev.*, vol. 3, no. 6, pp. 556–574, Nov. 2009.
[37] R. Raussendorf and H. J. Briegel, "A one-way quantum computer," *Phys. Rev. Lett.*, vol. 86, no. 22, pp. 5188–5191, May 2001.
[38] M. Cerezo. (Jun. 2019). *Entangled Physics: Quantum Information & Quantum Computation*. Accessed: Apr. 18, 2021. [Online]. Available: https://entangledphysics.com/2019/06/24/quantum-fidelity-or-how-to-compare-quantum-states/
[39] P. W. Shor, "Scheme for reducing decoherence in quantum computer memory," *Phys. Rev. A, Gen. Phys.*, vol. 52, pp. 2493–2496, Oct. 1995.
[40] E. Joos, *Decoherence*. Berlin, Germany: Springer, 2009, pp. 155–159.
[41] P. Krantz, M. Kjaergaard, F. Yan, T. P. Orlando, S. Gustavsson, and W. D. Oliver, "A quantum engineer's guide to superconducting qubits," *Appl. Phys. Rev.*, vol. 6, Jun. 2019, Art. no. 021318.
[42] G. Wendin, "Quantum information processing with superconducting circuits: A review," *Rep. Prog. Phys.*, vol. 80, no. 10, Sep. 2017, Art. no. 106001.
[43] E. Magesan, J. M. Gambetta, and J. Emerson, "Scalable and robust randomized benchmarking of quantum processes," *Phys. Rev. Lett.*, vol. 106, no. 18, May 2011, Art. no. 180504.
[44] J. I. Cirac and P. Zoller, "A scalable quantum computer with ions in an array of microtraps," *Nature*, vol. 404, no. 6778, pp. 579–581, Apr. 2000.
[45] K. Chen, C.-M. Li, Q. Zhang, Y.-A. Chen, A. Goebel, S. Chen, A. Mair, and J.-W. Pan, "Experimental realization of one-way quantum computing with two-photon four-qubit cluster states," *Phys. Rev. Lett.*, vol. 99, no. 12, Sep. 2007, Art. no. 120503sss.
[46] M. Hein, W. Dür, and H.-J. Briegel, "Entanglement properties of multipartite entangled states under the influence of decoherence," *Phys. Rev. A, Gen. Phys.*, vol. 71, no. 3, Mar. 2005, Art. no. 032350.
[47] T. Yang, Q. Zhang, J. Zhang, J. Yin, Z. Zhao, M. Żukowski, Z.-B. Chen, and J.-W. Pan, "All-versus-nothing violation of local realism by two-photon, four-dimensional entanglement," *Phys. Rev. Lett.*, vol. 95, no. 24, Dec. 2005, Art. no. 240406.
[48] G. Vallone, E. Pomarico, F. D. Martini, and P. Mataloni, "Active one-way quantum computation with two-photon four-qubit cluster states," *Phys. Rev. Lett.*, vol. 100, no. 16, Apr. 2008, Art. no. 160502.
[49] D. E. Browne and H. J. Briegel, "One-way quantum computation—A tutorial introduction," 2006, *arXiv:quant-ph/0603226*.
[50] J. Fulconis, O. Alibart, J. L. O'Brien, W. J. Wadsworth, and J. G. Rarity, "Nonclassical interference and entanglement generation using a photonic crystal fiber pair photon source," *Phys. Rev. Lett.*, vol. 99, no. 12, Sep. 2007, Art. no. 120501.
[51] S. M. Lee, H. S. Park, J. Cho, Y. Kang, J. Y. Lee, H. Kim, D.-H. Lee, and S.-K. Choi, "Experimental realization of a four-photon seven-qubit graph state for one-way quantum computation," *Opt. Exp.*, vol. 20, no. 7, p. 6915, Mar. 2012.
[52] S. Resch and U. R. Karpuzcu, "Quantum computing: An overview across the system stack," 2019, *arXiv:1905.07240*.
[53] K.-A. Suominen, "Physical implementation of large-scale quantum computation," in *Handbook of Natural Computing*. Berlin, Germany: Springer, 2012, pp. 1493–1520.
[54] F. Jazaeri, A. Beckers, A. Tajalli, and J.-M. Sallese, "A review on quantum computing: From qubits to front-end electronics and cryogenic MOSFET physics," in *Proc. 26th Int. Conf. Mixed Design Integr. Circuits Syst. (MIXDES)*, Jun. 2019, pp. 15–25.
[55] T. Xin, B.-X. Wang, K.-R. Li, X.-Y. Kong, S.-J. Wei, T. Wang, D. Ruan, and G.-L. Long, "Nuclear magnetic resonance for quantum computing: Techniques and recent achievements," *Chin. Phys. B*, vol. 27, no. 2, Feb. 2018, Art. no. 020308.
[56] O. Pfister, "Continuous-variable quantum computing in the quantum optical frequency comb," *J. Phys. B, At., Mol. Opt. Phys.*, vol. 53, no. 1, Nov. 2019, Art. no. 012001.
[57] T.-C. Wei, "Measurement-based quantum computation," 2021, *arXiv:2109.10111*.
[58] H. J. Briegel, D. E. Browne, W. Dür, R. Raussendorf, and M. Van den Nest, "Measurement-based quantum computation," *Nature Phys.*, vol. 5, pp. 19–26, Jan. 2009.
[59] M. A. Nielsen, "Cluster-state quantum computation," *Rep. Math. Phys.*, vol. 57, no. 1, pp. 147–161, Feb. 2006.
[60] R. Jozsa, "An introduction to measurement based quantum computation," *Quantum Information Processing-From Theory to Experiment* (NATO Science Series, III: Computer and Systems Sciences), vol. 199. 2006, pp. 137–158.
[61] R. Raussendorf, D. E. Browne, and H. J. Briegel, "Measurement-based quantum computation on cluster states," *Phys. Rev. A, Gen. Phys.*, vol. 68, no. 2, Aug. 2003, Art. no. 022312.

[62] R. Raussendorf and T.-C. Wei, "Quantum computation by local measurement," *Annu. Rev. Condens. Matter Phys.*, vol. 3, no. 1, pp. 239–261, Mar. 2012.

[63] H. J. Briegel and R. Raussendorf, "Persistent entanglement in arrays of interacting particles," *Phys. Rev. Lett.*, vol. 86, no. 5, pp. 910–913, Jan. 2001.

[64] M. W. Girard and G. Gour, "Entanglement monotones and transformations of symmetric bipartite states," *Phys. Rev. A, Gen. Phys.*, vol. 95, no. 1, Jan. 2017, Art. no. 012308.

[65] M. Van den Nest, A. Miyake, W. Dür, and H. J. Briegel, "Universal resources for measurement-based quantum computation," *Phys. Rev. Lett.*, vol. 97, no. 15, Oct. 2006, Art. no. 150504.

[66] M. V. D. Nest, W. Dür, A. Miyake, and H. J. Briegel, "Fundamentals of universality in one-way quantum computation," *New J. Phys.*, vol. 9, no. 6, p. 204, Jun. 2007.

[67] M. Hein, W. Dür, J. Eisert, R. Raussendorf, M. V. Nest, and H. J. Briegel, "Entanglement in graph states and its applications," in *Quantum Computers, Algorithms and Chaos* (Proceedings of the International School of Physics 'Enrico Fermi'). Varenna, Italy, vol. 162, Jul. 2005, doi: 10.3254/978-1-61499-018-5-115.

[68] C. M. Dawson, H. L. Haselgrove, and M. A. Nielsen, "Noise thresholds for optical cluster-state quantum computation," *Phys. Rev. A, Gen. Phys.*, vol. 73, no. 5, May 2006, Art. no. 052306.

[69] K. Fujii, "Stabilizer formalism and its applications," in *Quantum Computation with Topological Codes*. Singapore: Springer, 2015, pp. 24–55.

[70] D. Gottesman, "Stabilizer codes quantum error correction," Ph.D thesis, California Inst. Technol., Pasadena, CA, USA, May 1997.

[71] T. Chung, S. D. Bartlett, and A. C. Doherty, "Characterizing measurement-based quantum gates in quantum many-body systems using correlation functions," *Can. J. Phys.*, vol. 87, no. 3, pp. 219–224, 2009.

[72] M. Kashif and S. Al-Kuwari, "Qiskit as a simulation platform for measurement-based quantum computation," in *Proc. IEEE 19th Int. Conf. Softw. Archit. Companion (ICSA-C)*, Mar. 2022, pp. 152–159.

[73] N. C. Menicucci, P. van Loock, M. Gu, C. Weedbrook, T. C. Ralph, and M. A. Nielsen, "Universal quantum computation with continuous-variable cluster states," *Phys. Rev. Lett.*, vol. 97, no. 11, Sep. 2006, Art. no. 110501.

[74] X. Su, Y. Zhao, S. Hao, X. Jia, C. Xie, and K. Peng, "Experimental preparation of eight-partite cluster state for photonic qumodes," *Opt. Lett.*, vol. 37, no. 24, p. 5178, Dec. 2012.

[75] S. L. Braunstein, "Squeezing as an irreducible resource," *Phys. Rev. A, Gen. Phys.*, vol. 71, no. 5, May 2005, Art. no. 055801.

[76] S. B. Korolev, A. D. Manukhova, K. S. Tikhonov, T. Y. Golubeva, and Y. M. Golubev, "Criteria of minimum squeezing for quantum cluster state generation," *Laser Phys. Lett.*, vol. 15, no. 7, May 2018, Art. no. 075203.

[77] M. Gu, C. Weedbrook, N. C. Menicucci, T. C. Ralph, and P. van Loock, "Quantum computing with continuous-variable clusters," *Phys. Rev. A, Gen. Phys.*, vol. 79, no. 6, Jun. 2009, Art. no. 062318.

[78] M. V. Larsen, X. Guo, C. R. Breum, J. S. Neergaard-Nielsen, and U. L. Andersen, "Deterministic generation of a two-dimensional cluster state," *Science*, vol. 366, no. 6463, pp. 369–372, Oct. 2019.

[79] P. C. Humphreys, W. S. Kolthammer, J. Nunn, M. Barbieri, A. Datta, and I. A. Walmsley, "Continuous-variable quantum computing in optical time-frequency modes using quantum memories," *Phys. Rev. Lett.*, vol. 113, no. 13, Sep. 2014, Art. no. 130502.

[80] K. Liu, J. Guo, C. Cai, S. Guo, and J. Gao, "Experimental generation of continuous-variable hyperentanglement in an optical parametric oscillator," *Phys. Rev. Lett.*, vol. 113, no. 17, Oct. 2014, Art. no. 170501.

[81] M. Mamaev, R. Blatt, J. Ye, and A. M. Rey, "Cluster state generation with spin-orbit coupled fermionic atoms in optical lattices," *Phys. Rev. Lett.*, vol. 122, no. 16, Apr. 2019, Art. no. 160402.

[82] D. L. Zhou, B. Zeng, Z. Xu, and C. P. Sun, "Quantum computation based on d-level cluster state," *Phys. Rev. A, Gen. Phys.*, vol. 68, Dec. 2003, Art. no. 062303.

[83] I. Schwartz, D. Cogan, E. R. Schmidgall, Y. Don, L. Gantz, O. Kenneth, N. H. Lindner, and D. Gershoni, "Deterministic generation of a cluster state of entangled photons," *Science*, vol. 354, no. 6311, pp. 434–437, Oct. 2016.

[84] W. Asavanant, Y. Shiozawa, S. Yokoyama, B. Charoensombutamon, H. Emura, R. N. Alexander, S. Takeda, J.-I. Yoshikawa, N. C. Menicucci, H. Yonezawa, and A. Furusawa, "Generation of time-domain-multiplexed two-dimensional cluster state," *Science*, vol. 366, no. 6463, pp. 373–376, Oct. 2019.

[85] S. Yokoyama, R. Ukai, S. C. Armstrong, C. Sornphiphatphong, T. Kaji, S. Suzuki, J.-I. Yoshikawa, H. Yonezawa, N. C. Menicucci, and A. Furusawa, "Ultra-large-scale continuous-variable cluster states multiplexed in the time domain," *Nature Photon.*, vol. 7, no. 12, pp. 982–986, Nov. 2013.

[86] J.-I. Yoshikawa, S. Yokoyama, T. Kaji, C. Sornphiphatphong, Y. Shiozawa, K. Makino, and A. Furusawa, "Invited article: Generation of one-million-mode continuous-variable cluster state by unlimited time-domain multiplexing," *APL Photon.*, vol. 1, no. 6, Sep. 2016, Art. no. 060801.

[87] R. Yang, J. Wang, J. Zhang, K. Liu, and J. Gao, "Generation of continuous-variable spatial cluster entangled states in optical mode comb," *J. Opt. Soc. Amer. B, Opt. Phys.*, vol. 33, no. 12, pp. 2424–2429, 2016.

[88] R. N. Alexander, P. Wang, N. Sridhar, M. Chen, O. Pfister, and N. C. Menicucci, "One-way quantum computing with arbitrarily large time-frequency continuous-variable cluster states from a single optical parametric oscillator," *Phys. Rev. A, Gen. Phys.*, vol. 94, no. 3, Sep. 2016, Art. no. 032327.

[89] A. L. Grimsmo and A. Blais, "Squeezing and quantum state engineering with Josephson travelling wave amplifiers," *npj Quantum Inf.*, vol. 3, no. 1, p. 20, Jun. 2017.

[90] F. Albarrán-Arriagada, G. Alvarado Barrios, M. Sanz, G. Romero, L. Lamata, J. C. Retamal, and E. Solano, "One-way quantum computing in superconducting circuits," *Phys. Rev. A, Gen. Phys.*, vol. 97, no. 3, Mar. 2018, Art. no. 032320.

[91] O. Pfister, S. Feng, G. Jennings, R. Pooser, and D. Xie, "Multipartite continuous-variable entanglement from concurrent nonlinearities," *Phys. Rev. A, Gen. Phys.*, vol. 70, no. 2, Aug. 2004, Art. no. 020302.

[92] N. C. Menicucci, S. T. Flammia, and O. Pfister, "One-way quantum computing in the optical frequency comb," *Phys. Rev. Lett.*, vol. 101, no. 13, Sep. 2008, Art. no. 130501.

[93] C. Weedbrook, S. Pirandola, R. García-Patrón, N. J. Cerf, T. C. Ralph, J. H. Shapiro, and S. Lloyd, "Gaussian quantum information," *Rev. Modern Phys.*, vol. 84, no. 2, pp. 621–669, May 2012.

[94] A. Furusawa and P. V. Loock, *Introduction to Optical Quantum Information Processing*. Hoboken, NJ, USA: Wiley, 2011, ch. 2, pp. 79–123.

[95] M. Pysher, Y. Miwa, R. Shahrokhshahi, R. Bloomer, and O. Pfister, "Parallel generation of quadripartite cluster entanglement in the optical frequency comb," *Phys. Rev. Lett.*, vol. 107, no. 3, Jul. 2011, Art. no. 030505.

[96] M. Chen, N. C. Menicucci, and O. Pfister, "Experimental realization of multipartite entanglement of 60 modes of a quantum optical frequency comb," *Phys. Rev. Lett.*, vol. 112, no. 12, Mar. 2014, Art. no. 120505.

[97] P. Wang, W. Fan, and O. Pfister, "Engineering large-scale entanglement in the quantum optical frequency comb: Influence of the quasiphasematching bandwidth and of dispersion," 2015, *arXiv:1403.6631*.

[98] P. Wang, M. Chen, N. C. Menicucci, and O. Pfister, "Weaving quantum optical frequency combs into continuous-variable hypercubic cluster states," *Phys. Rev. A, Gen. Phys.*, vol. 90, no. 3, Sep. 2014, Art. no. 032325.

[99] S. Lloyd and S. L. Braunstein, "Quantum computation over continuous variables," *Phys. Rev. Lett.*, vol. 82, no. 8, pp. 1784–1787, Feb. 1999.

[100] N. C. Menicucci, "Fault-tolerant measurement-based quantum computing with continuous-variable cluster states," *Phys. Rev. Lett.*, vol. 112, no. 12, Mar. 2014, Art. no. 120504.

[101] T. C. Ralph, A. Gilchrist, G. J. Milburn, W. J. Munro, and S. Glancy, "Quantum computation with optical coherent states," *Phys. Rev. A, Gen. Phys.*, vol. 68, no. 4, Oct. 2003, Art. no. 042319.

[102] D. Gottesman, A. Kitaev, and J. Preskill, "Encoding a qubit in an oscillator," *Phys. Rev. A, Gen. Phys.*, vol. 64, no. 1, Jun. 2001, Art. no. 012310.

[103] Z. Y. Ou, S. F. Pereira, H. J. Kimble, and K. C. Peng, "Realization of the Einstein–Podolsky–Rosen paradox for continuous variables," *Phys. Rev. Lett.*, vol. 68, no. 25, pp. 3663–3666, Jun. 1992.

[104] D. F. Walls and G. J. Milburn, *Quantum Optics*. Berlin, Germany: Springer-Verlag, 2007.

[105] J. Zhang and S. L. Braunstein, "Continuous-variable Gaussian analog of cluster states," *Phys. Rev. A, Gen. Phys.*, vol. 73, no. 3, Mar. 2006, Art. no. 032318.

[106] C. M. Caves, K. S. Thorne, R. W. P. Drever, V. D. Sandberg, and M. Zimmermann, "On the measurement of a weak classical force coupled to a quantum-mechanical oscillator. I. Issues of principle," *Rev. Modern Phys.*, vol. 52, no. 2, pp. 341–392, Apr. 1980.

[107] B. Yurke, "Optical back-action-evading amplifiers," *J. Opt. Soc. Amer. B, Opt. Phys.*, vol. 2, no. 5, pp. 732–738, May 1985.

[108] Y. Miwa, J.-I. Yoshikawa, P. van Loock, and A. Furusawa, "Demonstration of a universal one-way quantum quadratic phase gate," *Phys. Rev. A, Gen. Phys.*, vol. 80, no. 5, Nov. 2009, Art. no. 050303.

[109] R. L. Barnes, "Stabilizer codes for continuous-variable quantum error correction," 2004, *arXiv:quant-ph/0405064*.

[110] P. van Loock, C. Weedbrook, and M. Gu, "Building Gaussian cluster states by linear optics," *Phys. Rev. A, Gen. Phys.*, vol. 76, no. 3, Sep. 2007, Art. no. 032321.

[111] J. Zhang, "Graphical description of local Gaussian operations for continuous-variable weighted graph states," *Phys. Rev. A, Gen. Phys.*, vol. 78, no. 5, Nov. 2008, Art. no. 052307.

[112] N. Bohr, "Can quantum-mechanical description of physical reality be considered complete?" *Phys. Rev.*, vol. 48, no. 8, pp. 696–702, Oct. 1935.

[113] A. Einstein, B. Podolsky, and N. Rosen, "Can quantum-mechanical description of physical reality be considered complete?" *Phys. Rev.*, vol. 47, no. 10, pp. 777–780, May 1935.

[114] X. Li, Q. Pan, J. Jing, J. Zhang, C. Xie, and K. Peng, "Quantum dense coding exploiting a bright Einstein–Podolsky–Rosen beam," *Phys. Rev. Lett.*, vol. 88, no. 4, Jan. 2002, Art. no. 047904.

[115] F. Grosshans, G. Van Assche, J. Wenger, R. Brouri, N. J. Cerf, and P. Grangier, "Quantum key distribution using Gaussian-modulated coherent states," *Nature*, vol. 421, no. 6920, pp. 238–241, Jan. 2003.

[116] A. Furusawa, J. L. Sørensen, S. L. Braunstein, C. A. Fuchs, H. J. Kimble, and E. S. Polzik, "Unconditional quantum teleportation," *Science*, vol. 282, no. 5389, pp. 706–709, Oct. 1998.

[117] H.-K. Lau and C. Weedbrook, "Quantum secret sharing with continuous-variable cluster states," *Phys. Rev. A, Gen. Phys.*, vol. 88, no. 4, Oct. 2013, Art. no. 042313.

[118] J.-I. Yoshikawa, Y. Miwa, A. Huck, U. L. Andersen, P. van Loock, and A. Furusawa, "Demonstration of a quantum nondemolition sum gate," *Phys. Rev. Lett.*, vol. 101, no. 25, Dec. 2008, Art. no. 250501.

[119] P. van Loock and A. Furusawa, "Detecting genuine multipartite continuous-variable entanglement," *Phys. Rev. A, Gen. Phys.*, vol. 67, no. 5, May 2003, Art. no. 052315.

[120] X. Zhu, C.-H. Chang, C. González-Arciniegas, A. Pe'er, J. Higgins, and O. Pfister, "Hypercubic cluster states in the phase-modulated quantum optical frequency comb," *Optica*, vol. 8, no. 3, p. 281, Mar. 2021.

[121] M. Yukawa, R. Ukai, P. van Loock, and A. Furusawa, "Experimental generation of four-mode continuous-variable cluster states," *Phys. Rev. A, Gen. Phys.*, vol. 78, no. 1, Jul. 2008, Art. no. 012301.

[122] N. C. Menicucci, S. T. Flammia, H. Zaidi, and O. Pfister, "Ultracompact generation of continuous-variable cluster states," *Phys. Rev. A, Gen. Phys.*, vol. 76, no. 1, Jul. 2007, Art. no. 010302.

[123] S. T. Flammia, N. C. Menicucci, and O. Pfister, "The optical frequency comb as a one-way quantum computer," *J. Phys. B, At., Mol. Opt. Phys.*, vol. 42, no. 11, May 2009, Art. no. 114009.

[124] M. Pysher, A. Bahabad, P. Peng, A. Arie, and O. Pfister, "Quasi-phase-matched concurrent nonlinearities in periodically poled $KTiOPO_4$ for quantum computing over the optical frequency comb," *Opt. Lett.*, vol. 35, pp. 565–567, Feb. 2010.

[125] M. Izutsu, S. Shikama, and T. Sueta, "Integrated optical SSB modulator/frequency shifter," *IEEE J. Quantum Electron.*, vol. QE-17, no. 11, pp. 2225–2227, Nov. 1981.

[126] H. Zaidi, N. C. Menicucci, S. T. Flammia, R. Bloomer, M. Pysher, and O. Pfister, "Entangling the optical frequency comb: Simultaneous generation of multiple 2×2 and 2×3 continuous-variable cluster states in a single optical parametric oscillator," *Laser Phys.*, vol. 18, no. 5, pp. 659–666, May 2008.

[127] N. C. Menicucci, "Temporal-mode continuous-variable cluster states using linear optics," *Phys. Rev. A, Gen. Phys.*, vol. 83, no. 6, Jun. 2011, Art. no. 062314.

[128] N. C. Menicucci, X. Ma, and T. C. Ralph, "Arbitrarily large continuous-variable cluster states from a single quantum nondemolition gate," *Phys. Rev. Lett.*, vol. 104, no. 25, Jun. 2010, Art. no. 250503.

[129] S. E. Economou, N. Lindner, and T. Rudolph, "Optically generated 2-dimensional photonic cluster state from coupled quantum dots," *Phys. Rev. Lett.*, vol. 105, no. 9, Aug. 2010, Art. no. 093601.

[130] M. D. Reid, P. D. Drummond, W. P. Bowen, E. G. Cavalcanti, P. K. Lam, H. A. Bachor, U. L. Andersen, and G. Leuchs, "*Colloquium*: The Einstein–Podolsky–Rosen paradox: From concepts to applications," *Rev. Modern Phys.*, vol. 81, no. 4, pp. 1727–1751, Dec. 2009.

[131] K. Fukui, W. Asavanant, and A. Furusawa, "Temporal-mode continuous-variable three-dimensional cluster state for topologically protected measurement-based quantum computation," *Phys. Rev. A, Gen. Phys.*, vol. 102, no. 3, Sep. 2020, Art. no. 032614.

[132] M. A. Nielsen, "Optical quantum computation using cluster states," *Phys. Rev. Lett.*, vol. 93, no. 4, Jul. 2004, Art. no. 040503.

[133] K. Liu, J. Guo, C. Cai, J. Zhang, and J. Gao, "Direct generation of spatial quadripartite continuous variable entanglement in an optical parametric oscillator," *Opt. Lett.*, vol. 41, pp. 5178–5181, Nov. 2016.

[134] J. Zhang, J. J. Wang, R. G. Yang, K. Liu, and J. R. Gao, "Large-scale continuous-variable dual-rail cluster entangled state based on spatial mode comb," *Opt. Exp.*, vol. 25, pp. 27172–27181, Oct. 2017.

[135] S. L. W. Midgley, A. S. Bradley, O. Pfister, and M. K. Olsen, "Quadripartite continuous-variable entanglement via quadruply concurrent down-conversion," *Phys. Rev. A, Gen. Phys.*, vol. 81, no. 6, Jun. 2010, Art. no. 063834.

[136] B. C. D. Santos, K. Dechoum, and A. Z. Khoury, "Continuous-variable hyperentanglement in a parametric oscillator with orbital angular momentum," *Phys. Rev. Lett.*, vol. 103, no. 23, Dec. 2009, Art. no. 230503.

[137] R. Pooser and J. Jing, "Continuous-variable cluster-state generation over the optical spatial mode comb," *Phys. Rev. A, Gen. Phys.*, vol. 90, no. 4, Oct. 2014, Art. no. 043841.

[138] J. Janousek, K. Wagner, J.-F. Morizur, N. Treps, P. K. Lam, C. C. Harb, and H.-A. Bachor, "Optical entanglement of co-propagating modes," *Nature Photon.*, vol. 3, no. 7, pp. 399–402, Jul. 2009.

[139] S. Armstrong, J.-F. Morizur, J. Janousek, B. Hage, N. Treps, P. K. Lam, and H.-A. Bachor, "Programmable multimode quantum networks," *Nature Commun.*, vol. 3, no. 1, pp. 1–8, Aug. 2012.

[140] C. Cai, L. Ma, J. Li, H. Guo, K. Liu, H. Sun, R. Yang, and J. Gao, "Generation of a continuous-variable quadripartite cluster state multiplexed in the spatial domain," *Photon. Res.*, vol. 6, pp. 479–484, May 2018.

[141] E. H. Huntington, G. N. Milford, C. Robilliard, T. C. Ralph, O. Glöckl, U. L. Andersen, S. Lorenz, and G. Leuchs, "Demonstration of the spatial separation of the entangled quantum sidebands of an optical field," *Phys. Rev. A, Gen. Phys.*, vol. 71, no. 4, Apr. 2005, Art. no. 041802.

[142] B.-H. Wu, R. N. Alexander, S. Liu, and Z. Zhang, "Quantum computing with multidimensional continuous-variable cluster states in a scalable photonic platform," *Phys. Rev. Res.*, vol. 2, no. 2, May 2020, Art. no. 023138.

[143] R. Yang, J. Zhang, I. Klich, C. González-Arciniegas, and O. Pfister, "Spatiotemporal graph states from a single optical parametric oscillator," *Phys. Rev. A, Gen. Phys.*, vol. 101, no. 4, Apr. 2020, Art. no. 043832.

[144] U. L. Andersen, J. S. Neergaard-Nielsen, P. Van Loock, and A. Furusawa, "Hybrid discrete- and continuous-variable quantum information," *Nature Phys.*, vol. 11, no. 9, pp. 713–719, 2015.

[145] R. F. Werner, "Quantum states with Einstein–Podolsky–Rosen correlations admitting a hidden-variable model," *Phys. Rev. A, Gen. Phys.*, vol. 40, no. 8, pp. 4277–4281, Oct. 1989.

[146] A. C. Doherty, P. A. Parrilo, and F. M. Spedalieri, "Distinguishing separable and entangled states," *Phys. Rev. Lett.*, vol. 88, no. 18, Apr. 2002, Art. no. 187904.

[147] M. Horodecki, P. Horodecki, and R. Horodecki, "Separability of mixed states: Necessary and sufficient conditions," *Phys. Lett. A*, vol. 223, nos. 1–2, pp. 1–8, Nov. 1996.

[148] A. Peres, "Separability criterion for density matrices," *Phys. Rev. Lett.*, vol. 77, no. 8, pp. 1413–1415, Aug. 1996.

[149] R. Horodecki, P. Horodecki, M. Horodecki, and K. Horodecki, "Quantum entanglement," *Rev. Mod. Phys.*, vol. 81, no. 2, pp. 865–942, 2009.

[150] R. Ukai, N. Iwata, Y. Shimokawa, S. C. Armstrong, A. Politi, J.-I. Yoshikawa, P. van Loock, and A. Furusawa, "Demonstration of unconditional one-way quantum computations for continuous variables," *Phys. Rev. Lett.*, vol. 106, no. 24, Jun. 2011, Art. no. 240504.

[151] P. Walther, K. J. Resch, T. Rudolph, E. Schenck, H. Weinfurter, V. Vedral, M. Aspelmeyer, and A. Zeilinger, "Experimental one-way quantum computing," *Nature*, vol. 434, no. 7030, pp. 169–176, Mar. 2005.

[152] G. M. D'Ariano, M. D. Laurentis, M. G. A. Paris, A. Porzio, and S. Solimeno, "Quantum tomography as a tool for the characterization of optical devices," *J. Opt. B, Quantum Semiclass. Opt.*, vol. 4, no. 3, pp. S127–S132, Jun. 2002.

[153] J. T. Barreiro, N. K. Langford, N. A. Peters, and P. G. Kwiat, "Generation of hyperentangled photon pairs," *Phys. Rev. Lett.*, vol. 95, no. 26, Dec. 2005, Art. no. 260501.

[154] G. Vallone, E. Pomarico, P. Mataloni, F. De Martini, and V. Berardi, "Realization and characterization of a two-photon four-qubit linear cluster state," *Phys. Rev. Lett.*, vol. 98, no. 18, May 2007, Art. no. 180502.

[155] B. P. Lanyon, M. Barbieri, M. P. Almeida, T. Jennewein, T. C. Ralph, K. J. Resch, G. J. Pryde, J. L. O'Brien, A. Gilchrist, and A. G. White, "Simplifying quantum logic using higher-dimensional Hilbert spaces," *Nature Phys.*, vol. 5, no. 2, pp. 134–140, Feb. 2009.

[156] W.-B. Gao, C.-Y. Lu, X.-C. Yao, P. Xu, O. Gühne, A. Goebel, Y.-A. Chen, C.-Z. Peng, Z.-B. Chen, and J.-W. Pan, "Experimental demonstration of a hyper-entangled ten-qubit Schrödinger cat state," *Nature Phys.*, vol. 6, no. 5, pp. 331–335, Mar. 2010.

[157] W.-B. Gao, P. Xu, X.-C. Yao, O. Gühne, A. Cabello, C.-Y. Lu, C.-Z. Peng, Z.-B. Chen, and J.-W. Pan, "Experimental realization of a controlled-NOT gate with four-photon six-qubit cluster states," *Phys. Rev. Lett.*, vol. 104, no. 2, Jan. 2010, Art. no. 020501.

[158] R. Ceccarelli, G. Vallone, F. De Martini, P. Mataloni, and A. Cabello, "Experimental entanglement and nonlocality of a two-photon six-qubit cluster state," *Phys. Rev. Lett.*, vol. 103, no. 16, Oct. 2009, Art. no. 160401.

[159] Y. Tokunaga, S. Kuwashiro, T. Yamamoto, M. Koashi, and N. Imoto, "Generation of high-fidelity four-photon cluster state and quantum-domain demonstration of one-way quantum computing," *Phys. Rev. Lett.*, vol. 100, no. 21, May 2008, Art. no. 210501.

[160] B. A. Bell, M. S. Tame, A. S. Clark, R. W. Nock, W. J. Wadsworth, and J. G. Rarity, "Experimental characterization of universal one-way quantum computing," *New J. Phys.*, vol. 15, no. 5, May 2013, Art. no. 053030.

[161] A. Clark, B. Bell, J. Fulconis, M. M. Halder, B. Cemlyn, O. Alibart, C. Xiong, W. J. Wadsworth, and J. G. Rarity, "Intrinsically narrowband pair photon generation in microstructured fibres," *New J. Phys.*, vol. 13, no. 6, Jun. 2011, Art. no. 065009.

[162] D. E. Browne and T. Rudolph, "Resource-efficient linear optical quantum computation," *Phys. Rev. Lett.*, vol. 95, no. 1, Jun. 2005, Art. no. 010501.

[163] T. P. Bodiya and L.-M. Duan, "Scalable generation of graph-state entanglement through realistic linear optics," *Phys. Rev. Lett.*, vol. 97, no. 14, Oct. 2006, Art. no. 143601.

[164] D. Bouwmeester, J.-W. Pan, M. Daniell, H. Weinfurter, and A. Zeilinger, "Observation of three-photon Greenberger–Horne–Zeilinger entanglement," *Phys. Rev. Lett.*, vol. 82, no. 7, pp. 1345–1349, Feb. 1999.

[165] C. A. Sackett, D. Kielpinski, B. E. King, C. Langer, V. Meyer, C. J. Myatt, M. Rowe, Q. A. Turchette, W. M. Itano, D. J. Wineland, and C. Monroe, "Experimental entanglement of four particles," *Nature*, vol. 404, no. 6775, pp. 256–259, Mar. 2000.

[166] H. Häffner, W. Hänsel, C. F. Roos, J. Benhelm, D. Chek-al-kar, M. Chwalla, T. Körber, U. D. Rapol, M. Riebe, P. O. Schmidt, C. Becher, O. Gühne, W. Dür, and R. Blatt, "Scalable multiparticle entanglement of trapped ions," *Nature*, vol. 438, no. 7068, pp. 643–646, Dec. 2005.

[167] R. Prevedel, G. Cronenberg, M. S. Tame, M. Paternostro, P. Walther, M. S. Kim, and A. Zeilinger, "Experimental realization of Dicke states of up to six qubits for multiparty quantum networking," *Phys. Rev. Lett.*, vol. 103, no. 2, Jul. 2009, Art. no. 020503.

[168] T. Monz, P. Schindler, J. T. Barreiro, M. Chwalla, D. Nigg, W. A. Coish, M. Harlander, W. Hänsel, M. Hennrich, and R. Blatt, "14-qubit entanglement: Creation and coherence," *Phys. Rev. Lett.*, vol. 106, no. 13, Mar. 2011, Art. no. 130506.

[169] W. Wieczorek, R. Krischek, N. Kiesel, P. Michelberger, G. Tóth, and H. Weinfurter, "Experimental entanglement of a six-photon symmetric Dicke state," *Phys. Rev. Lett.*, vol. 103, no. 2, Jul. 2009, Art. no. 020504.

[170] M. Rådmark, M. Żukowski, and M. Bourennane, "Experimental test of fidelity limits in six-photon interferometry and of rotational invariance properties of the photonic six-qubit entanglement singlet state," *Phys. Rev. Lett.*, vol. 103, no. 15, Oct. 2009, Art. no. 150501.

[171] P. G. Kwiat, K. Mattle, H. Weinfurter, A. Zeilinger, A. V. Sergienko, and Y. Shih, "New high-intensity source of polarization-entangled photon pairs," *Phys. Rev. Lett.*, vol. 75, no. 24, pp. 4337–4341, Dec. 1995.

[172] X.-C. Yao, T.-X. Wang, P. Xu, H. Lu, G.-S. Pan, X.-H. Bao, C.-Z. Peng, C.-Y. Lu, Y.-A. Chen, and J.-W. Pan, "Observation of eight-photon entanglement," *Nature Photon.*, vol. 6, no. 4, pp. 225–228, Feb. 2012.

[173] Y.-H. Kim, S. P. Kulik, M. V. Chekhova, W. P. Grice, and Y. Shih, "Experimental entanglement concentration and universal bell-state synthesizer," *Phys. Rev. A, Gen. Phys.*, vol. 67, no. 1, Jan. 2003, Art. no. 010301.

[174] W. Dür and J. I. Cirac, "Multiparticle entanglement and its experimental detection," *J. Phys. A, Math. Gen.*, vol. 34, no. 35, pp. 6837–6850, Aug. 2001.

[175] X.-L. Wang, L.-K. Chen, W. Li, H.-L. Huang, C. Liu, C. Chen, Y.-H. Luo, Z.-E. Su, D. Wu, Z.-D. Li, H. Lu, Y. Hu, X. Jiang, C.-Z. Peng, L. Li, N.-L. Liu, Y.-A. Chen, C.-Y. Lu, and J.-W. Pan, "Experimental ten-photon entanglement," *Phys. Rev. Lett.*, vol. 117, Nov. 2016, Art. no. 210502.

[176] H.-S. Zhong, Y. Li, W. Li, L.-C. Peng, Z.-E. Su, Y. Hu, Y.-M. He, X. Ding, W. Zhang, H. Li, L. Zhang, Z. Wang, L. You, X.-L. Wang, X. Jiang, L. Li, Y.-A. Chen, N.-L. Liu, C.-Y. Lu, and J.-W. Pan, "12-photon entanglement and scalable scattershot boson sampling with optimal entangled-photon pairs from parametric down-conversion," *Phys. Rev. Lett.*, vol. 121, no. 25, Dec. 2018, Art. no. 250505.

[177] X.-L. Wang, Y.-H. Luo, H.-L. Huang, M.-C. Chen, Z.-E. Su, C. Liu, C. Chen, W. Li, Y.-Q. Fang, X. Jiang, J. Zhang, L. Li, N.-L. Liu, C.-Y. Lu, and J.-W. Pan, "18-qubit entanglement with six photons' three degrees of freedom," *Phys. Rev. Lett.*, vol. 120, no. 26, Jun. 2018, Art. no. 260502.

[178] D. Istrati, Y. Pilnyak, J. C. Loredo, C. Antón, N. Somaschi, P. Hilaire, H. Ollivier, M. Esmann, L. Cohen, L. Vidro, C. Millet, A. Lemaître, I. Sagnes, A. Harouri, L. Lanco, P. Senellart, and H. S. Eisenberg, "Sequential generation of linear cluster states from a single photon emitter," *Nature Commun.*, vol. 11, no. 1, p. 5501, Oct. 2020.

[179] P. Senellart, G. Solomon, and A. White, "High-performance semiconductor quantum-dot single-photon sources," *Nature Nanotechnol.*, vol. 12, no. 11, pp. 1026–1039, Nov. 2017.

[180] Y. Pilnyak, N. Aharon, D. Istrati, E. Megidish, A. Retzker, and H. S. Eisenberg, "Simple source for large linear cluster photonic states," *Phys. Rev. A, Gen. Phys.*, vol. 95, Feb. 2017, Art. no. 022304.

[181] H.-L. Huang, D. Wu, D. Fan, and X. Zhu, "Superconducting quantum computing: A review," *Sci. China Inf. Sci.*, vol. 63, Jul. 2020, Art. no. 180501.

[182] Y. Wang, Y. Li, Z.-Q. Yin, and B. Zeng, "16-qubit IBM universal quantum computer can be fully entangled," *npj Quantum Inf.*, vol. 4, p. 46, Sep. 2018.

[183] J. A. Smolin, J. M. Gambetta, and G. Smith, "Efficient method for computing the maximum-likelihood quantum state from measurements with additive Gaussian noise," *Phys. Rev. Lett.*, vol. 108, no. 7, Feb. 2012, Art. no. 070502.

[184] G. J. Mooney, C. D. Hill, and L. C. L. Hollenberg, "Entanglement in a 20-qubit superconducting quantum computer," *Sci. Rep.*, vol. 9, no. 1, p. 13465, Sep. 2019.

[185] M. Gong et al., "Genuine 12-qubit entanglement on a superconducting quantum processor," *Phys. Rev. Lett.*, vol. 122, no. 11, Mar. 2019, Art. no. 110501.

[186] J. Koch, T. M. Yu, J. Gambetta, A. A. Houck, D. I. Schuster, J. Majer, A. Blais, M. H. Devoret, S. M. Girvin, and R. J. Schoelkopf, "Charge-insensitive qubit design derived from the Cooper pair box," *Phys. Rev. A, Gen. Phys.*, vol. 76, no. 4, Oct. 2007, Art. no. 042319.

[187] G. J. Mooney, G. A. L. White, C. D. Hill, and L. C. L. Hollenberg, "Generation and verification of 27-qubit Greenberger–Horne–Zeilinger states in a superconducting quantum computer," *J. Phys. Commun.*, vol. 5, no. 9, Sep. 2021, Art. no. 095004.

[188] F. B. Maciejewski, Z. Zimborás, and M. Oszmaniec, "Mitigation of readout noise in near-term quantum devices by classical post-processing based on detector tomography," *Quantum*, vol. 4, p. 257, Apr. 2020.

[189] G. J. Mooney, G. A. L. White, C. D. Hill, and L. C. L. Hollenberg, "Whole-device entanglement in a 65-qubit superconducting quantum computer," *Adv. Quantum Technol.*, vol. 4, no. 10, Oct. 2021, Art. no. 2100061.

[190] K. X. Wei, I. Lauer, S. Srinivasan, N. Sundaresan, D. T. McClure, D. Toyli, D. C. McKay, J. M. Gambetta, and S. Sheldon, "Verifying multipartite entangled Greenberger–Horne–Zeilinger states via multiple quantum coherences," *Phys. Rev. A, Gen. Phys.*, vol. 101, no. 3, Mar. 2020, Art. no. 032343.
[191] S. Takeda, T. Mizuta, M. Fuwa, P. van Loock, and A. Furusawa, "Deterministic quantum teleportation of photonic quantum bits by a hybrid technique," *Nature*, vol. 500, no. 7462, pp. 315–318, Aug. 2013.
[192] M. Ho, O. Morin, J.-D. Bancal, N. Gisin, N. Sangouard, and J. Laurat, "Witnessing single-photon entanglement with local homodyne measurements: Analytical bounds and robustness to losses," *New J. Phys.*, vol. 16, no. 10, Oct. 2014, Art. no. 103035.
[193] H. Jeong, A. Zavatta, M. Kang, S.-W. Lee, L. S. Costanzo, S. Grandi, T. C. Ralph, and M. Bellini, "Generation of hybrid entanglement of light," *Nature Photon.*, vol. 8, no. 7, pp. 564–569, Jul. 2014.
[194] K. Nemoto and W. J. Munro, "Nearly deterministic linear optical controlled-NOT gate," *Phys. Rev. Lett.*, vol. 93, no. 25, Dec. 2004, Art. no. 250502.

MUHAMMAD KASHIF received the bachelor's degree in electrical (electronics) engineering from the COMSATS Institute of Information Technology, Pakistan, in 2015, and the master's degree in electronics and computer engineering from Istanbul Sehir University, Istanbul, Turkey, in 2019. He is currently a Ph.D. Scholar with the College of Science and Engineering, Hamad Bin Khalifa University, Qatar. His research interests include hardware security, quantum computing, and quantum machine learning.

SAIF AL-KUWARI (Senior Member, IEEE) received the Bachelor of Engineering degree in computers and networks from the University of Essex, U.K., in 2006, and the dual Ph.D. degree in computer science from the University of Bath and Royal Holloway, University of London, U.K., in 2012. He is currently an Assistant Professor with the College of Science and Engineering, Hamad Bin Khalifa University. His research interests include quantum computing, cryptography, computational forensics, and their connections with machine learning. He is a fellow of IET and BCS and a Senior Member of ACM.